Published in final edited form as:
Dev Biol. 2010 October 1; 346(1): 25–38. doi:10.1016/j.ydbio.2010.07.008.

O-Fucosylation of Thrombospondin Type 1 Repeats Restricts Epithelial to Mesenchymal Transition (EMT) and Maintains Epiblast Pluripotency During Mouse Gastrulation

Jianguang Du[1], **Hideyuki Takeuchi**[1], **Christina Leonhard-Melief**[1], **Kenneth R. Shroyer**[2], **Malgosia Dlugosz**[1], **Robert S. Haltiwanger**[1,*], and **Bernadette C. Holdener**[1,*]

[1] Department of Biochemistry and Cell Biology, Institute for Cell and Developmental Biology, Center for Developmental Genetics, Stony Brook University, Stony Brook, NY 11794-5215

[2] Department of Pathology, Stony Brook University, Stony Brook, NY 11794-8691

Abstract

Thrombospondin type 1 repeat (TSR) superfamily members regulate diverse biological activities ranging from cell motility to inhibition of angiogenesis. In this study, we verified that mouse protein *O*-fucosyltransferase-2 (POFUT2) specifically adds *O*-fucose to TSRs. Using two *Pofut2* gene trap lines, we demonstrated that *O*-fucosylation of TSRs was essential for restricting epithelial to mesenchymal transition in the primitive streak, correct patterning of mesoderm, and localization of the definitive endoderm. Although *Pofut2* mutant embryos established anterior/posterior polarity, they underwent extensive mesoderm differentiation at the expense of maintaining epiblast pluripotency. Moreover, mesoderm differentiation was biased towards the vascular endothelial cell lineage. Localization of *Foxa2* and *Cer1* expressing cells within the interior of *Pofut2* mutant embryos suggested that POFUT2 activity was also required for the displacement of the primitive endoderm by definitive endoderm. Notably, *Nodal, BMP4, Fgf8*, and *Wnt3* expression were markedly elevated and expanded in *Pofut2* mutants, providing evidence that *O*-fucose modification of TSRs was essential for modulation of growth factor signaling during gastrulation. The ability of *Pofut2* mutant embryos to form teratomas comprised of tissues from all three germ layer origins suggested that defects in *Pofut2* mutant embryos resulted from abnormalities in the extracellular environment. This prediction is consistent with the observation that POFUT2 targets are constitutive components of the extracellular matrix (ECM) or associate with the ECM. For this reason, the *Pofut2* mutants represent a valuable tool for studying the role of *O*-fucosylation in ECM synthesis and remodeling, and will be a valuable model to study how post-translational modification of ECM components regulates the formation of tissue boundaries, cell movements, and signaling.

[*]Authors for correspondence: bernadette.holdener@stonybrook.edu and robert.haltiwanger@stonybrook.edu.

Competing Interest

The authors have no financial, personal, or professional interests that could be construed to have influenced this paper.

Financial Disclosure

A grant from the National Institutes of Health to RSH and BCH (CA12307101) supported these studies. The funding agency had no role in role in study design, data collection and analysis, decision to publish, or preparation of the manuscript.

Keywords

Gastrulation; Thrombospondin type I repeat; Epithelial to Mesenchymal Transition; Extracellular Matrix; *O*-fucose; Protein *O*-fucosyltransferase

Introduction

Epidermal growth factor-like (EGF) and thrombospondin type 1 repeats (TSRs) can be modified by an unusual form of *O*-linked glycosylation called *O*-fucose [1,2,3]. EGF repeats and TSRs are 40–60 aa cysteine-rich motifs found in a wide variety of cell surface and secreted proteins. TSRs are somewhat larger than EGF repeats, but both contain six conserved cysteines forming three disulfide bonds, although the disulfide bonding patterns for each are distinct [2]. *O*-Fucose is added to EGF repeats by protein *O*-fucosyltransferase 1 (POFUT1) [4], while POFUT2 *O*-fucosylates TSRs [5,6]. Both enzymes are highly selective, modifying only properly folded repeats containing the appropriate consensus sequences [2]. The similarity between *Notch* and *Pofut1* mutant phenotypes in mice and *Drosophila* provides evidence that the *O*-fucose residues on the Notch receptor EGF repeats are essential for its function [7,8]. Cell biological and biochemical studies investigating the role of *O*-fucose on Notch also support this view [9,10,11,12]. Further evidence for the importance of *O*-fucose glycans in Notch function comes from the observation that Fringe, a known modulator of Notch function, functions by adding a β3-linked *N*-acetylglucosamine to *O*-fucose residues on the EGF repeats of Notch [2,13,14].

POFUT2 is closely related to POFUT1, but modifies TSRs that contain the consensus sequence: C-$X_{2–3}$-(S/T)-C-X_2-G, where the cysteines are the first and second conserved cysteines in group 1 TSRs, or the second and third cysteines in group 2 TSRs (Table 1) [1,5,6,15,16,17, 18]. *O*-Fucose on TSRs can be elongated by a β 3-glucosyltransferase [19,20]. In humans, the failure to add β 3-linked glucose to *O*-fucose on TSRs results in Peter's Plus Syndrome, an autosomal recessive disorder characterized by developmental delay, anterior eye chamber defects, and cleft palate [20,21,22], suggesting that *O*-fucosylation of TSR-containing proteins will be critical for their function.

Examination of the SMART database for TSR proteins containing the POFUT2 consensus recognition sequence identified 51 putative targets in mice (Table 1). Among these potential targets, the number of TSRs predicted to be modified by POFUT2 varies considerably. Putative POFUT2 targets include 10 transmembrane proteins and 41 secreted proteins that regulate diverse cellular processes including cell differentiation, proliferation, adhesion, migration, apoptosis, extracellular matrix (ECM) production, angiogenesis, nerve development, innate immune response, regional patterning of vascular system, and cleavage of plasma Von Willebrand factor [23,24,25,26,27,28,29,30,31,32]. Moreover the receptor binding, signal modulating, and anti-angiogenic function of several putative POFUT2 target proteins is attributed to the TSRs [33,34,35,36,37,38,39].

Given the precedent for the role of *O*-fucose modification of EGF repeats in Notch receptor function, and the importance of TSRs for protein function, we predict that the *O*-fucose modification of TSRs will also be important for the biological roles of POFUT2 target proteins. Furthermore, since many POFUT2 target proteins, including CCN, TSP, and ADAMTS family members, are involved in ECM synthesis and remodeling or modulation of growth factor signaling, we hypothesized that loss of POFUT2 activity could disrupt embryonic processes such as gastrulation, which require controlled regulation of growth factor signaling and matrix remodeling [40,41]. To determine the role of POFUT2 in mouse embryo development, we characterized the biochemical specificity of mouse POFUT2 and the effects of two gene trap

disruptions of *Pofut2*. These data demonstrated that TSR *O*-fucosylation was important for maintaining organized tissues in the pre-gastrula embryo. Importantly, loss of *Pofut2* resulted in unrestricted epithelial to mesenchymal transition (EMT) and biased differentiation of vascular endothelial cells. Widespread expression of *Nodal, BMP, Wnt3* and *Fgf8* in *Pofut2* mutant embryos suggested that *O*-fucose modification of TSRs was critical for maintaining a balance of signaling within the embryo.

Materials and Methods

Ethics statement

All animal work was conducted according to relevant national and international guidelines. Stony Brook University operates under Assurance #A3011-01, approved by the NIH Office of Laboratory Animal Welfare (OLAW) (OLAW). The animal studies were approved by the Institutional Animal Care and Use and Committee (IACUC) which follow all the guidance set forth in: Public Health Service Policy on Humane Care and Use of Laboratory Animals distributed by Office of Laboratory Animal Welfare, NIH; Animal Welfare Act and Animal Welfare Regulations distributed by United States Department of Agriculture; and Guide for the Care and Use of Laboratory Animals distributed by the National Research Council. Stony Brook University animal facilities are accredited with AAALAC International (Association for the Assessment and Accreditation of Laboratory Animal Care International).

Generation of Pofut2 Expression constructs

Mouse POFUT2 cDNA was amplified by PCR from a mouse testis cDNA library (a kind gift from Dr. William J. Lennarz) with the primers, Forward: 5′-CATATCATAAAGCTTGCCATGGCGGCGCTCAGCGTCGTCTGC-3′, and Reverse: 5′-CATATATATCTCGAGGTACGCAATCTTCCAGTGTGTGGGCTG-3′, and digested with Hind III and Xho I, and cloned into pcDNA4/TO/myc-His vector (Invitrogen). Since this construct does not contain the Pofut2 stop codon, recombinant proteins will be expressed as myc and His_6 tagged proteins (POFUT2-Myc-His). For the expression of untagged mouse POFUT2, the *Pofut2* cDNA (including stop codon) was inserted between Hind III and Xba I sites of pcDNA4 (Invitrogen). To mutate the ERE motif (POFUT2/E396A-myc-His), site-directed mutagenesis was carried out to replace dA at 1187 (nt) with dC.

Transient transfection and Purification of the myc- and 6x His-tagged POFUT2 protein by Ni-NTA chromatography

HEK293T cells were transiently transfected with the expression plasmids encoding full-length mouse *Pofut2* with or without myc- and hexa-His- tags at its C-terminus (*Pofut2-myc-His*), or the empty plasmid pcDNA4 as control by Lipofectamine 2000 (Invitrogen). Culture medium (5 ml) of the transiently transfected cells was dialyzed against 50 mM Tris-HCl pH 7.4 containing 25% glycerol overnight. The dialyzed sample was mixed with 200 μl of the 50% slurry pre-equilibrated Ni-NTA agarose (QIAGEN), rotated at 4°C for 1 hour, and poured into the Poly-Prep Chromatography Columns (BIO-RAD). The resin was washed with 50 mM Tris-HCl pH 7.4 containing 25% glycerol and 0.5 M NaCl, and then with 50 mM Tris-HCl pH 7.4 containing 25% glycerol and 10 mM imidazole. The tagged proteins were eluted with 50 mM Tris-HCl pH 7.4 containing 25% glycerol and 250 mM imidazole. The imidazole in the sample was removed by gel filtration on Sephadex G50 (SIGMA). Protein concentration of the tagged protein was determined by Coomassie staining of samples separated by SDS-PAGE using BSA as a standard. After collection of the culture media, the transfected cells were harvested and, homogenized in 50 mM Tris-HCl pH 7.4 buffer containing protease inhibitors, 10 mM $MgCl_2$, and 250 mM NaCl, by Polytron homogenizer for 15 sec, and then incubated at 4°C for 1 hour. After the homogenate was centrifuged at 16,000x g for 20 min, the supernatant was

collected as cell extracts and kept at −80°C until use. Protein concentration was determined by a BCA assay using BSA as a standard.

Preparation of TSR and EGF Repeats

The third TSR from human thrombospondin 1 (TSP1-TSR3 was expressed in bacteria and purified as described previously [6]. The first EGF repeat of human factor VII was a kind gift of Dr. Yang Wang [42]. Protein concentration was determined by a BCA assay using BSA as a standard.

Preparation of tissue extracts from adult mice

Tissues of 5-week-old wildtype and heterozygous male mice were dissected and homogenized in 0.5 ml (approximately 5 volume of tissue sample) of 50 mM Tris-HCl pH 7.4 buffer containing protease inhibitors, 10 mM $MgCl_2$, and 250 mM NaCl, by Polytron homogenizer for 15 sec, and then incubated at 4°C for 1 hour. The supernatant was collected from tissue extracts after centrifugation at 16,000x g for 20 min and kept at −80°C until use. Protein concentration was determined by BCA assay using BSA as a standard.

Protein O-fucosyltransferase assays

POFUT2 assays were performed with slight modification as previously described [6]. Briefly, 10 μl reaction mixture contained 50 mM HEPES pH 7.0, 10 mM $MnCl_2$, 10 μM TSR, 2.9 μM (0.05 mCi/ml) GDP-[^{3}H]fucose, 50 μM GDP-fucose, 0.5% NP-40, and 7 μl of tissue extracts. The POFUT1 assays were essentially the same with the POFUT2 assays except that the factor VII EGF instead of TSR was used at a concentration of 10 μM as acceptor substrates. The reaction was incubated at 37°C for 20 min and stopped by adding 900 μl of 100 mM EDTA pH 8.0. The sample was loaded onto a C18 cartridge (100 mg, Agilent). After the cartridge was washed with 5 ml of H_2O, the TSR or EGF repeat was eluted with 1 ml of 80% methanol. Incorporation of [^{3}H]fucose into the TSR or EGF repeat was determined by scintillation counting of the eluates. Reactions without substrates were used as background control.

Mice and genotyping

The *Pofut2*$^{Gt(RST434)Byg}$ transgenic mice were generated with stem cell clone RST434 (BayGenomics) at the UC-Davis transgenic facility. For simplicity, we will refer to this allele as *RST434* throughout the manuscript. For genotyping, three primers were designed: RST434-forward (GAGGCCGGGAGTACTGGGAT) matches sequence of *Pofut2* exon 5, RST434-reverse1 (ATCTTCGTCCAGTCTTCCTCC) matches the sequence of *Pofut2* exon 6 that was deleted by the insertion of gene trap vector, and RST434-reverse2 (GGTTGCCAGAACCAGCAAACTGAA) matches the En2 exon sequence in the gene trap vector pGT0TMpfs. RST434-forward and RST434-reverse1 were used to amplify the wildtype allele-specific band of 955 bp, whereas RST434-forward and RST434-reverse2 amplify the genetrap insertion-specific band of 1344 bp.

The *Pofut2*$^{Gt(neo)699Lex}$ transgenic mice were purchased from Lexicon Genetics Incorporated. For simplicity this allele will be referred to as *699Lex* throughout the manuscript. For genotyping, 1197-upper (GATCTTAAGTTCCAGCGAGACA) and LTR-rev2 (ATAAACCCTCTTGCAGTTGCATC) were used to amplify the mutant allele band of 600 bp. 1197-upper and 1197-3′ (GCCTCACTGTGATATTACAGGTCC) were used to amplify the wildtype allele band of 314 bp. Mice heterozygous for both *699Lex* and Bat-gal (*699Lex*/+;BAT-gal/+) were generated by crossing the *Pofut2*$^{Gt(neo)699Lex}$ transgenic mice with BAT-gal transgene reporter [43]. The BAT-gal reporter gene was confirmed by PCR with lacZ-up (CGGTGATGGTGCTGCGTTGGA) and lacZ-down (ACCACCGCACGATAGAGATTC) that amplify 385 bp of the β-galactosidase cDNA.

LacZ staining and Histology

Embryos in decidua were stained with X-gal as described [44]. Briefly, decidua at E 6.5 and E 7.5 were fixed with 0.2% glutaraldehyde for 25 min and 30 min respectively followed by 3 times of rinses with detergent rinse (15 min for each rinse). The decidua were then stained at 37°C for 20 hrs. After staining, decidua were rinsed in 0.1M phosphate buffer pH7.3 for 15min followed by post fixation with 4% paraformaldehyde in 0.1M phosphate buffer pH7.3. Embryos were subsequently dissected out from deciduas, cleared in 80% glycerol, and photographed. For sectioning, either the embryo in decidua or isolated embryos were then embedded in paraffin and sectioned. The slides were mounted with Gel Mount (Sigma) for LacZ staining photography and then the cover slips were removed after soaking in water for 24 hrs. The slides were subsequently stained with hematoxylin and eosin Y and mounted with Permount (Fisher) for photomicroscopy. The BAT-gal embryos were fixed with 4% paraformaldehyde in PBS pH7.3 at 4°C for 1 hr followed by X-gal staining at 37°C for 20 hrs. The embryos were postfixed at room temperature for 10 min, cleared, and photographed.

Whole-mount embryo in situ hybridization

The *in situ* hybridization was carried out as previously described in [45]. To reduce trapping in E 7.5 *Pofut2* mutant embryos, tissues were perforated with a tungsten needle. For each gene analyzed, *in situ* hybridization was carried out with both sense and anti-sense probes. The cDNAs of *Foxa2*, *Sox2*, and *Gooscoid* were amplified from E7.5 mouse embryo cDNA and were cloned into pBluescript SK(−) between Xho I and Not I sites. Primers used for cDNA amplification are listed in Supplementary Table 3. Other DNA constructs for probe preparation were kindly provided by Drs. Bernhard Herrman (*T*), Brigid Hogan (*Bmp4*), Janet Rossant (*Kdr*(*flk1)* and *eomesodermin*), Hans Scholer (*Pou5fa*), Stephen Frankenberg (*Cubilin*), Michael M Shen (*Nodal, Lefty1*, and *Lefty2*), Gail Martin (*Fgf8*), Rosa Beddington (*Cer1*), Richard Behringer (*Wnt3*), Virginia Papaioannou (*Tbx6*), Nancy Speck (*Runx1*) and Thomas Gridley (*Snail*).

To genotype the in situ embryos, the embryos were rehydrated and the crosslinks were reversed in 200mM NaOH at 60°C overnight before adding lysis buffer (200mg/ml proteinase K, 10mM DTT, 50mM KCl, 1.5mM $MgCl_2$, 10mM Tris HCl pH8.5, 0.01% gelatin, 0.45% NP-40, 0.45% Tween-20). Embryo lysates were boiled for 5 minutes and used directly for PCR. Pofut2-probe-p (5′-GGATCCTAATACGACTCACTATAGGGAGGAAGACTGGACGAAGAT-3′) and Pofut2-gen-down1 (5′-AAGGAAACCCAGCTTTGAGGAGGA-3′) were used to amplify the wildtype band, and LacZ-up (5′-CGGTGATGGTGCTGCGTTGGA-3′) and LacZ-down (5′-ACCACCGCACGATAGAGATTC-3′) were used to amplify the mutant band.

RT-PCR analysis

For *Pofut2* expression at adult stage, total RNA from tissues of 5-week-old males was isolated with Trizol reagent (Invitrogen) and was reverse transcribed with Oligo(dT)12-18 primers. Primers used for the semi-quantitative PCR include: Pofut2 forward (5′-TGTACTCGCAGGACAAGCATGAGT-3′) and Pofut2 reverse (5′-AACATGATCTCGAGTCAGTACGCAATCTTCCAGTGTGTG-3′) were used to amplify *Pofut2*. GAPDH reverse (5′-ACCACAGTCCATGCCATCAC-3′) and GAPDH forward (5′-TCCACCACCCTGTTGCTGTA-3′) were used to amplify the glyceraldehyde 3-phosphate dehydrogenase (*Gapdh*) cDNA as standards for normalizing samples. Briefly, input of reverse transcription product of different tissues was adjusted to give equal amount of *Gapdh* PCR product within the linear range of PCR amplification. Subsequently, the adjusted amount of reverse transcription reaction was used for PCR using *Pofut2* primers. For the expression of putative POFUT2 target proteins and matrix metalloproteinase-2 and -9, total RNA was isolated from E 7.5 wildtype embryos and was reverse transcribed with random primers (Invitrogen). PCR was carried out with gene specific primers (Supplementary Table 1). To

avoid amplification of genomic DNA, the primer pairs span at least one intron. Positive control PCR was carried out with complementary DNA randomly transcribed from total RNAs of adult brain and spleen.

Real time PCR

Total RNA was isolated from E 7.5 homozygous mutant embryos, and E 7.5 wildtype plus heterozygous embryos. Total RNAs were then reverse transcribed using random primers (Invitrogen). Real time PCR was carried out using SYBER Green I Master Mix (Roche). GAPDH was used as endogenous control. The primers of genes tested are listed in Supplementary Table 2. No significant signal was detected when total RNA was used as template.

Immunohistochemistry

For Amnionless, embryos were fixed in 4% paraformaldehyde and embedded in paraffin. Embryo sections (~7 μm) were stained with rabbit anti-mouse Amnionless (gift from Dr. Elizabeth Lacy) followed by biotinylated anti-rabbit and Vectastain elite ABC kit (Vector laboratories). The peroxidase staining was subsequently developed using DAB (diaminobenzidine). For PECAM-1, E-cadherin, and Laminin-1 immunostaining, embryos were fixed with zinc fixative (BD Pharmingen) at room temperature for 24 hrs followed by paraffin embedding and sectioning. Immunostaining was carried out with rat anti-mouse PECAM-1 (clone MEC 13.3, BD Pharmingen), Rabbit anti-E-cadherin mAb (24E10, Cell Signaling), Rabbit polyclonal anti-laminin (Sigma), Alexa Fluor® 488 goat anti-rat IgG (Molecular Probes), and Alexa Fluor® 488 goat anti-rabbit IgG (Molecular Probes). The images of Laminin were taken with Axio Imager Z1 (Carl Zeiss) and those of PECAM-1 and E-cadherin were taken with confocal microscope (LSM 510 Meta NLO, Carl Zeiss). Final pictures were exported as stacked images of 7 sequential 1 μM scans with LSM Image Browser and AxioVision Rel. 4.6.

Mouse teratoma surgery

The surgery was carried out as described [46]. Briefly, the E7.5 embryos were implanted into testis of wildtype mice. The testes were dissected 8 weeks after transplantation surgery and sectioned followed by *hematoxylin and eosin Y staining.*

O-dianisidine staining of hemoglobin

Hemoglobin-containing cells in E 8.5 embryos were detected by O-dianisidine staining as described by O'Brien [47], with the following modifications: embryos were stained for 1 hour followed by water wash. The embryos were then washed with 1X PBS followed by postfix with 4% paraformaldehyde in PBS for overnight at 4°C. The embryos were then washed with 1X PBS and cleared with 80% glycerol for photography. Parietal endoderm was removed from some mutant embryos before staining. No difference was seen for mutant embryos with or without parietal endoderm.

Results

Mouse POFUT2 has TSR-specific *O*-fucosyltransferase activity

Recombinant *Drosophila* protein *O*-fucosyltransferase-2 (Ofut2) transfers fucose from GDP-fucose to a bacterially expressed TSR *in vitro* [5]. In addition, several mammalian cell lines contain endogenous TSR-specific *O*-fucosyltransferase activity [5,16,18]. To determine whether mouse POFUT2 behaves similarly, we expressed and purified POFUT2 (POFUT2-myc-His) and assayed its ability to *O*-fucosylate the third TSR (TSR3) of human thrombospondin 1 (TSP1) (Figure 1). *O*-Fucosylation of TSP1-TSR3 increased linearly with

increasing amount of POFUT2-myc-His (Figure 1A), donor substrate GDP-[^{3}H] fucose (Figure 1B), and TSR (Figure 1D). Combined, these results indicated that mouse POFUT2 has TSR-specific *O*-fucosyltransferase activity dependent on the concentration of both acceptor and donor substrates.

Protein *O*-fucosyltransferases contain a conserved DXD-like motif (Asp-X-Asp) believed to be crucial for the function of many classes of glycosyltransferases [48]. Disrupting this motif in *Drosophila* OFUT2 abrogates its activity [6]. An ERE-motif (Glu-Arg-Glu), similar to the conserved DXD-like motif, is present in mouse POFUT2. To test whether the ERE was also essential for mouse POFUT2 function, we substituted alanine for the first glutamic acid of the ERE motif (POFUT2/E396A-myc-His) and tested whether it could modify TSP1-TSR3 (Figures 1C and D). POFUT2 activity was detected in both culture media and cell extract of cells transfected with *Pofut2-myc-His* or untagged *Pofut2* (Figure 1C top panel). Although POFUT2 is normally localized to the endoplasmic reticulum (ER), secretion of some POFUT2 into the medium is observed upon expression (Figure 1C) [6,16]. No POFUT2 activity was detected in either culture medium or cell extracts of cells transfected with *Pofut2/E396A-myc-His* despite the presence of this fusion protein (Figure 1C, middle panel). To exclude the possibility that the loss of TSR *O*-fucosylation activity was caused by decreased expression of POFUT2/E396A-myc-His compared to POFUT2-His, *O*-fucosyltransferase assays were carried out *in vitro* with equal amount of purified protein (Figure 1D). In this assay, POFUT2-myc-His activity increased with increasing concentration of TSP1-TSR3. In contrast, no activity was detected for POFUT2/E396A-myc-His. These results provided convincing evidence that the ERE motif is essential for the protein *O*-fucosyltransferase activity of mouse POFUT2.

Gene trap disruption of *Pofut2* abrogates TSR *O*-fucosylation

Our bioinformatic analysis identified 51 mouse TSR-containing proteins that could potentially be *O*-fucosylated by POFUT2 (Table 1). These TSR superfamily members are widely expressed and play multiple roles in cell culture and in the adult [2,23,24,25,26,27,28,29,30,31,32,49]. Similarly, we observed wide spread expression of *Pofut2* in adult tissues (Supplementary Figure 1A). To investigate the biological role of POFUT2 in mice, we characterized two *Pofut2* gene trap insertions*: Pofut2*$^{Gt(RST434)Byg}$ (*RST434*) and *Pofut2*$^{Gt(neo)699Lex}$ (*699Lex*) (Figure 2A and Supplementary Figure 2A, respectively). The *RST434* genetrap was identified in an insertional mutagenesis screen to identify components of/or proteins traversing the secretory pathway [50]. This is consistent with the prediction that POFUT2 resides in the endoplasmic reticulum [6].

The *RST434* insertion occurred within exon 6 and resulted in an in-frame fusion between *Pofut2* (exons 1 through 5) and β-gal-neomycin (POFUT2-β-geo) (Figure 2A, Supplementary Figure 1B, and BayGenomics). Because the ERE motif essential for the POFUT2 activity is encoded by exon 9 (Figure 2A), we predicted that the POFUT2-β-geo fusion protein would lack TSR-specific *O*-fucosyltransferase activity. For this reason, the gene-trap provides a mechanism for disrupting *Pofut2* gene function as well as a mechanism for reporting *Pofut2* gene expression patterns. Consistent with this prediction, we detected half the activity of POFUT2 in *RST434* heterozygous cells compared with parent cells (Figure 2B). In contrast, no significant difference in POFUT1 activity was observed. POFUT2 activity was also reduced in extracts of adult tissues obtained from *RST434* heterozygotes relative to wild type animals, while POFUT1 activity was largely unaltered (Figure 2C). Combined, these data provided evidence that the *RST434* allele produced an enzymatically inactive protein.

Because the *RST434* gene-trap insertion resulted in a transmembrane fusion protein that contained 235 amino acids of POFUT2 protein fused to β-geo, the formal possibility existed that the fusion protein retained residual function other than enzymatic activity. For this reason,

we characterized a second gene trap allele, *699Lex*, produced by insertion of a retroviral vector VICTR48 into the first intron of *Pofut2* (Supplementary Figure 2A). Our RT-PCR analysis identified a fusion transcript including exon 1 of *Pofut2* and neomycin phosphotransferase (Supplementary Figure 2B). Tissues obtained from animals heterozygous for the *699Lex* gene trap insertion showed reduction in POFUT2 activity similar to that observed in *RST434* animals (Supplementary Figure 2C). Combined, these results provided convincing evidence that gene traps in both strains inactivate one copy of the *Pofut2* gene. For this reason, we anticipated that *RST434* and *699Lex Pofut2* insertions created null alleles and were valuable tools to determine the function of *O*-fucose modification of TSR-containing proteins.

Pofut2 is essential for organization of epithelia in pre-gastrula embryos

Consistent with the predicted importance of sugar modification for the function of TSR-containing proteins, no homozygous *RST434* animals were obtained from heterozygous intercrosses (Table 2). In contrast, heterozygotes (*RST434/+)* and wild type (+/+) animals were present in 2:1 ratio at weaning. Heterozygotes showed no overt pathologies and had similar lifespan to wild type littermates. These results provided evidence that *RST434* disruption of *Pofut2* results in either peri- or pre-natal lethality. To distinguish between these possibilities, we collected and genotyped embryos from intercrosses at mid-gestation (E 10.5) (Table 2). Heterozygotes and wild type embryos were present at the expected 2:1 ratio. Although no homozygous embryos were detected, resorption sites were present at a frequency expected for the homozygotes. Since resorption sites are indicative of embryo implantation and subsequent failure, these data suggested that homozygous embryos died after implantation and before E 10.5, a time period during which gastrulation and early organogenesis occurs.

We took advantage of the *Pofut2-β-geo* fusion to characterize *Pofut2* gene expression as well as identify homozygous mutants at the onset of gastrulation (E 6.5) (Figure 2). *RST434* homozygous embryos were distinguished from wildtype or heterozygous littermates by the intensity of LacZ staining (Figure 2D-F). We attributed the increased staining to the presence of two copies of the *Pofut2-β-geo* fusion and confirmed the genotype by PCR (Figure 2Di-Fi). LacZ activity, reflecting *Pofut2* expression, was detected in both embryonic and extra-embryonic tissues (including extraembryonic ectoderm, ectoplacental cone, and visceral and parietal endoderm) of heterozygous and mutant embryos (Figure 2E–F), with increased activity in the embryonic ectoderm. These data suggested that expression of *Pofut2* was elevated in this tissue relative to that of the visceral and parietal endoderm or extra-embryonic ectoderm.

At E 6.5, *RST434* homozygous embryos were distinguished subtly from wildtype and heterozygous littermates by their rounder appearance, shortened proximal-distal axis, and constriction in the junction between the extra-embryonic ectoderm and the ectoplacental cone (Compare Figure 2D and E with F). To evaluate the tissue composition of mutant embryos, we examined sagittal sections of embryos stained for LacZ activity (Figure 2G and H) followed by staining with hematoxylin and eosin Y (Figure 2Gi and Hi). At E 6.5, heterozygous littermates had well-differentiated ectoplacental cone, and embryonic and extra-embryonic ectoderm surrounded by visceral and parietal endoderm (Figure 2G, Gi). The composition of tissues in homozygous embryos appeared similar (Figure 2H, Hi). However, the mutant embryo was rounder, the embryonic and extra-embryonic ectoderm appeared thickened and disorganized, and there was a constriction between the extra-embryonic ectoderm and ectoplacental cone. This constriction appears to result from abnormal arrangement of the parietal and/or visceral endoderm. Combined, these subtle differences suggested that POFUT2 activity was not essential for specification of early cell lineages, epithelialization, and formation of the proamniotic cavity in the early post-implantation embryo, but was required for maintaining the organization of these tissues in the pre-gastrula embryo.

Pofut2 is required to restrict expression of signaling molecules early in gastrulation

To determine whether loss of *Pofut2* was required for establishment of polarity or for the onset of gastrulation, we looked at gene expression in embryos isolated from *RST434* heterozygous intercrosses at E 6.5 (Figure 3). By E 6.5, the wild type embryo established anterior posterior polarity and is poised to begin gastrulation (Figure 3, left embryos). Tissue identity as well as embryo polarity is evidenced by localized expression of *Cer1* and *Lefty1* in the anterior visceral endoderm (AVE) (Figure 3A and B), *Nodal, Wnt3, Fgf8, T* and *Eomes* in the primitive streak (Figure 3C–D, F–H), and *Eomes* and *Bmp4* in the extra-embryonic ectoderm (Figure 3H, I). Wnt signaling activity (Figure 3E) is similar to *Wnt3* mRNA expression and was detected using the BAT-gal transgene in embryos from the 699Lex. Similarly, we detected asymmetric and tissue specific expression of *Cer1, Lefty1, Nodal, Wnt3, Fgf8, T, Eomes* and *BMP4* and Wnt activity in all *RST434* homozygous littermates examined (Figure 3, right embryo). Because correct localization of the AVE is essential for the posterior localization of primitive streak makers, we do not believe that the apparent thickening of the extraembryonic endoderm layers observed at the distal tip of some *Pofut2* mutant embryos (Figure 3E, F, and I) results from the failure of the AVE cells to migrate, but rather results from physical constraints that prevent tissue expansion or movement. Combined, these results demonstrated that *O*-fucosylation of TSRs was not essential for establishment of polarity or initiation of gastrulation.

In contrast to *wildtype* littermates, the expression of *Nodal* and *Wnt3* was significantly expanded and/or displaced in the primitive streak and expression of *BMP4* was significantly expanded in the extra-embryonic ectoderm of *Pofut2* mutant embryos. Since cross-talk between Nodal, BMP, and Wnt signaling pathways is essential for maintaining normal expression of these genes [40], the expanded expression of the major growth factors in *Pofut2* mutants suggested that failure to *O*-fucosylate TSR-containing proteins disrupted the balance of signaling in the pre-gastrula/early gastrula. For this reason, we predicted that loss of *Pofut*2 would result in altered mesoderm patterning and/or gastrulation defects.

Pofut2 is required to maintain epiblast pluripotency and restrict EMT during gastrulation

By E7.5, gastrulation was well underway, and the *RST434* wildtype and heterozygous embryos were easily distinguished from homozygotes (Figure 4). In unaffected embryos (Figure 4A–C, left and D top), the embryonic and extra-embryonic ectoderm were organized into regular epithelia. The primitive streak, localized at the posterior, had reached its full length and a well-organized mesoderm layer was present. Further, extra-embryonic structures containing mesoderm derivatives (amnion, chorion, and allantois) had formed. *Pofut2* expression, as detected by LacZ activity, was similar to that observed at E 6.5, with elevated expression in the distal half of the embryo and additional expression in the mesoderm (Figure 4A–C, left).

In contrast, *RST434* homozygous embryos were unusually dense in appearance, shorter, and characterized by a dumb-bell shape (Figure 4A–C, right). The ectoplacental cone of mutants easily separated from the embryo. The embryonic ectoderm was present but thicker in structure and not organized into regular epithelia. The extra-embryonic ectoderm was similarly disorganized and separated from the ectoplacental cone by a constriction of visceral and parietal endoderm. In addition, Reichert's membrane comprised of parietal endoderm cells and ECM failed to expand in *RST434* homozygotes, and remained tightly associated with the visceral endoderm. Although *Pofut2* mutants lacked organized tissues comprised of mesoderm, mesenchymal cells were abundant, albeit considerably disorganized compared to unaffected embryos (Figure 4A–D). In addition, the region of the epiblast undergoing EMT transition appeared broader compared with wild type littermates (compare Figure 4D, top and bottom). We observed similar abnormalities in *699Lex* homozygotes and *699Lex/RST434* compound heterozygotes (Table 2 and Supplementary Figure 2D–G), providing further evidence that the gene trap insertions resulted in null *Pofut2* alleles.

Despite the morphological evidence for a primitive streak and the abundance of mesenchymal cells in *Pofut2* mutants, we failed to detect significant expression of the *Eomes, T,* and *Tbx6* in *Pofut2* mutants above background (Figure 4E–G, right; confirmed using real time PCR, Supplementary Figure 3). In *wildtype* embryos, *Eomes, T,* and *Tbx6,* are expressed in partially overlapping domains within the primitive streak and nascent mesoderm at E 7.5 (Figure 4E–G). In contrast, expression of *Snail1,* a classic marker of EMT and newly formed mesoderm during gastrulation, was markedly expanded in *Pofut2* mutants (Figure 4J, right) compared to *wildtype* littermates (Figure 4J, left). These results suggest that lack of *Eomes, T,* and *Tbx6* expression resulted from reduced cell contact within the *Pofut2* mutant primitive streak, rather than to a lack of mesoderm differentiation. Together, these data suggested that the *Pofut2* mutant epiblast was actively undergoing EMT and that the loose cells were differentiated mesoderm (Figure 4J, right). Consistent with this prediction, we observed a marked reduction in the expression of epiblast pluripotency markers, *Oct4* and *Sox2,* in *Pofut2* mutants compared to the wildtype embryos (Figure 4H–I).

To confirm that *Pofut2* mutant epiblast was undergoing active EMT, we characterized laminin and E-cadherin expression. In wildtype embryos, laminin is decreased in the region of the primitive streak undergoing EMT, compared to levels in surrounding epiblast (Figure 5A–B). In addition, E-cadherin expression is down regulated in the primitive streak cells undergoing EMT and the mesoderm (Figure 5E–F, and Ei-Fi). In *Pofut2* mutant embryos, the region of decreased laminin expression was slightly expanded compared to wildtype embryos (Figure 5C, D), corresponding to the region of reduced cell contact. Moreover, E-cadherin expression was markedly decreased throughout the *Pofut2* mutant epiblast (Figure 5G–H and Gi-Hi). These results were consistent with the elevation of *Snail1,* a negative regulator of *E-cadherin,* in the *Pofut2* mutants. Combined, the expansion of *Snail1* expression, decrease in E-cadherin expression, and the abundance of mesenchymal cells in *Pofut2* mutant embryos provided strong evidence that *O*-fucosylation of TSR proteins was essential to restrict EMT within the primitive streak and maintain epiblast pluripotency.

Pofut2 is essential for intercalation of definitive endoderm

Despite the formation of a primitive streak and mesoderm differentiation in *Pofut2* mutants, we did not observe a morphological node, the anterior organizing center of the primitive streak. For this reason, we examined the expression of major signals important for primitive streak patterning and markers of node derivatives in E 7.5 embryos. Consistent with our observations at E 6.5, we detected a marked expansion of *Nodal, Wnt3, BMP4,* and *Fgf8* expression, expanded Wnt activity detected by activation of the BAT-gal reporter, and a decrease in *Lefty2* expression in *Pofut2* mutants compared to wild type littermates (Figure 6A–F and Supplementary Figure 3). Expression of markers characteristic of both posterior mesoderm (*Flk1/Kdr*) as well as anterior mesendoderm (*Gsc*) were expanded in *Pofut2* mutants (Figure G and H), suggesting that loss of *Pofut2* did not block the patterning of the most anterior and posterior mesoderm, but rather affected the abundance of these cells. In addition, we detected expression of the definitive endoderm markers *Foxa2* and *Cer1* (Figure 6I and J). These results were consistent with specification of anterior mesendoderm derivatives in mutants, despite the absence of a morphological node. However, in contrast to wild type littermates, *Foxa2* and *Cer1* expressing cells remained within the interior of *Pofut2* mutants, and did not intercalate into the overlying visceral endoderm. The failure of *Foxa2* and *Cer1* expressing cells to displace the visceral endoderm in *Pofut2* mutants suggested that *O*-fucosylation of TSRs was essential for directing their localization.

Loss of POFUT2 promotes ectopic differentiation of vascular endothelial cells

In addition to defects in the *Pofut2* mutant epiblast, primitive streak and node derivatives, we observed abnormalities in the organization of the parietal and visceral endoderm layers

surrounding the embryonic and extraembryonic ectoderm. The proximal visceral endoderm overlying the extra-embryonic ectoderm is an absorptive epithelial and is characterized by expression of *Cubn* and Amn; these markers are normally down regulated in the more squamous visceral endoderm overlying the distal embryonic ectoderm (Figure 4K and L). Curiously, in *Pofut2* mutant embryos we observed expression of *Cubn* and Amn overlying the epiblast (Figure 4K and L). In a co-culture assay, proximal visceral endoderm can induce differentiation of blood from anterior epiblast, normally fated to become neural tissue [51]. For this reason, the distal expansion of the proximal visceral endoderm raises the possibility that defects in definitive endoderm localization could result in part from defective interactions with the visceral endoderm. In addition, we predict that altered characteristics of the visceral endoderm could dramatically impact the characteristics of the differentiating mesoderm.

Consistent with this prediction, we observed gross alteration in the characteristics of the *Pofut2* mutant mesoderm by E 8.5. At this time, wild type embryos had undergone gastrulation, neurulation, and began organogenesis (Figure 7A – Bi). Although the *Pofut2* mutant embryos had increased in size, they showed no morphological evidence of neurulation or organogenesis. In addition, clearly defined extraembryonic- and embryonic ectoderm-derived epithelial structures were lost by E 8.5 (Figure 7C – Di). In contrast, the mesenchymal cells in *Pofut2* mutants appeared to have condensed against the visceral endoderm, producing a structure bearing some resemblance to the visceral yolk sac (compare Figure 7Bi and Di). In wildtype embryos, the visceral yolk sac develops from proximal visceral endoderm and posterior mesoderm. Posterior mesoderm is characterized by the expression of the VEGF-receptor encoded by *Flk1* (Figure 6G and [52,53]). A subset of these cells will become the extra-embryonic mesoderm precursors of hematopoietic and endothelial cells in the yolk sac blood islands [52,54,55].

In wild-type embryos, *Flk1* expressing cells of the gastrula-staged mouse embryo differentiate into vascular endothelial cells (distinguished by PECAM1 staining) and primitive erythroid cells (characterized by morphology or O-dianisidine staining which detects hemoglobin) (Figure 7B, Bi, E, and G) [52,56]. Despite the abundance of *Flk1* expressing cells in *Pofut2* mutant embryos, there was no morphological evidence for primitive erythroid cells in *Pofut2* mutants nor did mutant embryos stain with O-dianisidine (Figure 7C–Di, and H). In contrast, vascular endothelial cells, marked by PECAM1 expression, were abundant throughout all but the most distal region of *Pofut2* mutants (Figure 7F, Fi, and Supplement Figure 4). The abundance of *Flk1* and PECAM1 positive cells and absence of differentiated primitive erythrocytes suggested that *O*-fucosylation of TSR proteins by POFUT2 was important for the distinction between the hematopoietic and vascular endothelial cell lineages.

The extracellular environment influences the potential of *Pofut2* mutant cells to differentiate

We identified 51 mouse TSR-containing proteins containing the consensus sequence for *O*-fucosylation by POFUT2 (Table 1). Using semi-quantitative RT-PCR, we detected transcripts encoding all but 10 putative POFUT2 targets at E 7.5 (Supplementary Table 1). Since POFUT2 facilitates the secretion of target proteins in cell culture experiments (e.g. ADAMTS13 and ADAMTSL1, [16,18]), the limited capacity for *Pofut2* mutant cells to differentiate within the embryo could stem from secretion defects of POFUT2 targets. However, the establishment of anterior/posterior polarity, which is dependent upon BMP, Nodal, and Wnt (not direct POFUT2 targets) signaling pathways provided indirect evidence that secretion was generally unaffected by the *Pofut2* mutation. Since many POFUT2 target proteins interact with the ECM or are constitutive components of ECM, the limited capacity for differentiation of *Pofut2* mutants more likely resulted from a defect in the extracellular environment or the ability of mutant cells to interact with the environment resulting specifically from absence or altered function of a POFUT2 target(s).

To test this hypothesis, we evaluated the ability of E 7.5 mutant embryos to differentiate in teratomas, where the ECM was provided in part by the environment of the testis (Figure 8). Wild type teratomas (n=6) ranged in diameter from 4633 μm to 9819 μm, with the exception of one tumor which only reached 2994 μm in diameter (data not shown). In contrast, *Pofut2* mutant embryos (n=6) formed smaller tumors ranging in size from 551 μm to 4279 μm in diameter. The smaller size suggested a potential cell-autonomous affect on cell proliferation or viability. Although smaller in size, the tissue composition of teratomas was comparable to those derived from wild type littermates, and contained tissues derived from all three germ layers (Figure 8A–F). The ability of *Pofut2* epiblast to differentiate into teratomas containing a variety of tissues not present in mutant embryos suggested that POFUT2 targets in the extracellular environment rather than cell surface localized-targets or intracellular POFUT2 function was essential for maintaining the pluripotency of the epiblast and influence the patterning of mesoderm.

Discussion

Loss of *Pofut2* disrupted cell differentiation as well as tissue morphology, boundaries, and relationships during gastrulation. Our biochemical studies demonstrated that POFUT2 specifically adds *O*-fucose to TSRs. The majority of predicted POFUT2 targets are constitutive components of the ECM or secreted matrix associated proteins capable of influencing cell adhesion/migration, ECM synthesis and remodeling, and modulating growth factor signaling (Table 1). This observation was consistent with the ability of *Pofut2* mutant cells to differentiate in the teratoma assay. For this reason, we hypothesize that loss of TSR *O*-fucosylation resulted in ECM changes that affected gastrulation by modulating growth factor signaling activity and/or altering or restricting cell movement [41].

The gross alteration in the tissue composition of the *Pofut2* mutant embryos demonstrated that *Pofut2* was a key modulator of gastrulation. During gastrulation the timing, activity, and distribution of growth factor signals must be fine-tuned to generate a diverse array of tissues within defined regions of the embryo. *Nodal* signaling is central to specification of anterior/posterior polarity, primitive streak formation, and mesoderm patterning [40,57,58]. In addition, there is considerable cross talk between the Nodal, BMP, and Wnt signaling pathways during specification of polarity and mesodermal cell fate [40,59]. Several known and predicted POFUT2 target proteins, including CCN2 (CTGF), CCN6 (WISP3), TSP1, ADAMTS1, ADAMTS8, and ADAMTSL2 negatively modulate the activity of TGFβ, BMP, WNT, FGF, BMP4 and VEGF signaling pathways [60,61,62,63,64,65]. The potential contribution of these proteins to the *Pofut2* phenotype is discussed in greater detail below.

The potential importance of *O*-fucosylation of TSRs in regulating TGFβ signaling is underscored by the identification of two amino acid substitutions in the TSRs of ADAMTSL2 in geleophysic dysplasia patients, characterized by brachydactyly, cardiac valvular abnormalities, and short stature [66]. These mutations are within the 6th and 7th TSRs containing conserved sequence for POFUT2 modification. Importantly, increased TGFβ and nuclear localization of phospho-SMAD2 are detected in cells isolated from geleophysic dysplasia patients, suggesting that ADAMTSL2 functions as a negative modulator of TGFβ signaling [66]. In addition, in *Xenopus* overexpression of another potential POFUT2 target, CCN2 (CTGF), antagonizes BMP signaling, but potentiates low-level TGFβ signaling [60].

Pofut2 mutants shared some phenotypic similarities to mutations that disturb the Nodal (a TGFβ) pathway. Expansion of gene expression characteristic of the proximal/posterior primitive streak is also observed in *Smad2*, *Nodal-NR* (precursor processing mutant), and *Drap1* mutant embryos. However, in *Smad2* and *Nodal-NR* mutant embryos, the failure to localize the primitive streak to the posterior results from the inability to specify and localize

the AVE and establish anterior/posterior polarity [57,67]. In contrast, *Pofut2* mutant embryos correctly localized the AVE and initially restricted expression of primitive streak markers to the posterior, suggesting that the expansion of markers did not result from a reduction of Nodal signaling or processing of the Nodal precursor or a failure to establish anterior/posterior polarity. In contrast, embryos lacking *Drap1*, encoding a transcriptional co-repressor, are predicted to enhance expression of *Nodal* [68]. *Drap1* mutants are characterized by an expansion of posterior localized *Nodal* transcripts, loss of *Brachyury (T)* and *Lefty2*, enlarged primitive streak, and excess EMT [68]. We observed similar defects in *Pofut2* mutant embryos, suggesting that the expansion of primitive streak and EMT in *Pofut2* mutants could be attributed in part to elevation of Nodal signalling. However, despite the similarities between *Pofut2* and *Drap1* mutants, differences in the organization of epithelia and pattern of mesoderm migration between *Pofut2* and *Drap1* mutants, suggested that defects in *Pofut2* mutant embryos were not limited to aberrant Nodal signaling.

Likely, loss of TSR *O*-fucosylation also causes changes in ECM composition that alter cell and/or tissue characteristics [41]. Reichert's membrane consisting of parietal endoderm cells and a dense sheet-like ECM comprised predominantly of laminin-1, collagen type IV, and heparan sulfate proteolgycan, was one of the earliest tissues affected in *Pofut2* mutants [25, 29,69,70,71]. Normally, Reichert's membrane is physically separated from the visceral endoderm, and the parietal endoderm cells are found widely spaced. In contrast, in *Pofut2* mutants this membrane was tightly associated with the visceral endoderm and the parietal endoderm cells were densely packed. These observations suggested that TSR *O*-fucosylation was essential for expansion of this membrane. The tight association between Reichert's membrane and the visceral endoderm likely placed considerable physical constraints on the developing *Pofut2* mutant embryo. In *Xenopus* development, increasing mechanical tension promotes early fibronectin fibril assembly and alters tissue characteristics [72]. For this reason, we predict that tension induced alterations in the ECM composition/organization could contribute to the irregular epithelia and abnormal cell differentiation and movement/migration observed in *Pofut2* mutants.

Gastrulation abnormalities in *Pofut2* mutant embryos also resulted in the distal expansion of the proximal visceral endoderm. It is unclear whether this expansion resulted from a distal expansion of visceral endoderm with proximal characteristics, or alternatively resulted from altered gene expression in the distal visceral endoderm. However, as a result the embryonic mesoderm was juxtaposed to a tissue that normally influences the differentiation of proximal/posterior extra-embryonic mesoderm [51,73]. For this reason, gain of inductive signals from the expanded proximal visceral endoderm in combination with the observed increase in *Bmp4* expression could contribute in to the expansion of posterior (*Flk1+*) mesoderm in *Pofut2* mutants. This prediction is supported by the observation that co-culture of proximal visceral endoderm and anterior epiblast results in the expression of BMP4 and in differentiation of blood precursors rather than differentiation of neural tissue in explants [51,73].

Although the *Flk1+* hemangioblasts of *wildtype* embryos have potential to develop into both vascular endothelial and blood lineages, *Pofut2* mutants lacked primitive erythrocytes despite an abundance of PECAM positive endothelial-like cells. In cell culture, high levels of FGF can inhibit primitive erythroid differentiation and promote endothelial cell fate [74]. For this reason, we predict that the elevated expression of *Fgf8* in *Pofut2* mutants likely influenced the differentiation of *Flk1+* cells into vascular endothelial cells. Other POFUT2 targets that could influence differentiation of the hemangioblast include ADAMTS1, ADAMTS8, and TSP1, as these proteins negatively modulate FGF and VEGF signaling [37,62,65,75]. ADAMTS8 and TSP1 both inhibit both VEGF and Fgf2 induced vascularization in culture assays; and inhibition of angiogenesis by TSP1 is proposed to result from the sequestering Fgf2 in the ECM by TSP1 TSRs [37].

Altered composition of the ECM could affect cell adhesion and migration within the gastrulating embryo and contribute to the excessive EMT. ADAMTS and TSP family members are POFUT2 targets that regulate ECM synthesis and remodeling [29,76,77,78,79,80,81]. The TSRs of these proteins are essential for proper protein function [34,36]. Thrombospondins 1 and 2 work indirectly to alter ECM by promoting endocytosis of the zymogens metalloproteinase (MM) MMP2 and MMP9 [82], which are expressed at E 7.5 (RT-PCR data not shown). In contrast, the ADAMTS proteins are metalloproteinases capable of directly remodeling ECM. Some ADAMTS family members cleave the chondroitin sulfate proteoglycans aggrecan and versican [25], shown to be mediators of EMT during embryoid body differentiation [83]. Unlike the *Pofut2* mutants, TSP1, ADAMTS4, and ADAMTS5 knockouts, and ADAMTS4/5 double knockouts are all viable [84,85,86,87].

CCN members (also POFUT2 targets) modulate cell adhesion by binding to integrins and heparin sulfate proteoglycans [79]. CCN2-deficient mouse embryonic fibroblasts (MEFs) do not adhere well to fibronectin and show delays in cell spreading [88]. Disruption of CCN6 in human mammary epithelial cells increased SNAIL and decreased expression of E-cadherin, a phenotype remarkably similar to *Pofut2* mutant embryos [89]. Although none of the single *Ccn* disruptions characterized thus far result in phenotypes similar to *Pofut2* mutants [90,91, 92,93,94], given the high degree of amino acid identity between CCN members (30–50%), it is likely that some CCN cellular functions overlap [79].

Our data clearly demonstrated that *Pofut2* was required during mouse gastrulation to coordinate morphogenetic movements and specify a range of tissues in the mouse embryo. These abnormalities underscored the importance of this unusual *O*-fucose post-translational modification for TSR protein function. Of the 51 proteins predicted to be modified by POFUT2, most were expressed during mouse gastrulation (Supplementary Table 1). To date, published knockouts of known or predicted targets of POFUT2 do not result in phenotypes similar to the *Pofut2* gene traps. These observations open the possibility that the *Pofut2* mutant phenotype could result from the combined loss-of-function or modulation of several of TSR family members. Because TSR proteins play critical roles in ECM composition, cell adhesion and migration, and cell signaling, we predict that tissue abnormalities and gastrulation defects in *Pofut2* mutants likely stem from altered signaling as well as altered physical properties of the ECM. For this reason, *Pofut2* mutant embryos, or embryonic stem cells derived from mutant embryos, not only represent a valuable tool for studying the role of *O*-fucosylation in ECM synthesis and remodeling, but also provide a model to study how ECM composition regulates the formation of tissue boundaries, cell movements, and signaling during gastrulation and other developmental processes, such as hematopoiesis and angiogenesis.

Supplementary Material

Refer to Web version on PubMed Central for supplementary material.

Acknowledgments

We wish to thank Richard Grady for exceptional technical assistance and Drs. Howard Sirotkin, Gerald Thomsen, Nurit Ballas, and William Gillis and members of our laboratories for critical reading of the manuscript.

Abbreviations

ADAMTS	A disintegrin and metalloproteinase with thrombospondin type 1 motif
CCN	Cyr, Ctgf, Nov
EGF	Epidermal growth factor-like

EMT	Epithelial to mesenchymal transition
ECM	Extracellular Matrix
POFUT	Protein *O*-fucosyltransferase
RST434	*Pofut2*$^{Gt(RST434)Byg}$
699Lex	*Pofut2*$^{Gt(neo)699Lex}$
TSR	Thrombospondin Type 1 repeat
TSP	Thrombospondin

References

1. Hofsteenge J, Huwiler KG, Macek B, Hess D, Lawler J, et al. C-mannosylation and O-fucosylation of the thrombospondin type 1 module. J Biol Chem 2001;276:6485–6498. [PubMed: 11067851]
2. Luther KB, Haltiwanger RS. Role of unusual O-glycans in intercellular signaling. Int J Biochem Cell Biol 2009;41:1011–1024. [PubMed: 18952191]
3. Moloney DJ, Shair LH, Lu FM, Xia J, Locke R, et al. Mammalian Notch1 is modified with two unusual forms of O-linked glycosylation found on epidermal growth factor-like modules. J Biol Chem 2000;275:9604–9611. [PubMed: 10734111]
4. Wang Y, Shao L, Shi S, Harris RJ, Spellman MW, et al. Modification of epidermal growth factor-like repeats with O-fucose. Molecular cloning and expression of a novel GDP-fucose protein O-fucosyltransferase. J Biol Chem 2001;276:40338–40345. [PubMed: 11524432]
5. Luo Y, Koles K, Vorndam W, Haltiwanger RS, Panin VM. Protein O-fucosyltransferase 2 adds O-fucose to thrombospondin type 1 repeats. J Biol Chem 2006;281:9393–9399. [PubMed: 16464857]
6. Luo Y, Nita-Lazar A, Haltiwanger RS. Two distinct pathways for O-fucosylation of epidermal growth factor-like or thrombospondin type 1 repeats. J Biol Chem 2006;281:9385–9392. [PubMed: 16464858]
7. Okajima T, Irvine KD. Regulation of notch signaling by o-linked fucose. Cell 2002;111:893–904. [PubMed: 12526814]
8. Shi S, Stanley P. Protein O-fucosyltransferase 1 is an essential component of Notch signaling pathways. Proc Natl Acad Sci U S A 2003;100:5234–5239. [PubMed: 12697902]
9. Okajima T, Xu A, Irvine KD. Modulation of notch-ligand binding by protein O-fucosyltransferase 1 and fringe. J Biol Chem 2003;278:42340–42345. [PubMed: 12909620]
10. Rampal R, Arboleda-Velasquez JF, Nita-Lazar A, Kosik KS, Haltiwanger RS. Highly conserved O-fucose sites have distinct effects on Notch1 function. J Biol Chem 2005;280:32133–32140. [PubMed: 15994302]
11. Sasamura T, Sasaki N, Miyashita F, Nakao S, Ishikawa HO, et al. neurotic, a novel maternal neurogenic gene, encodes an O-fucosyltransferase that is essential for Notch-Delta interactions. Development 2003;130:4785–4795. [PubMed: 12917292]
12. Stahl M, Uemura K, Ge C, Shi S, Tashima Y, et al. Roles of Pofut1 and O-fucose in mammalian Notch signaling. J Biol Chem 2008;283:13638–13651. [PubMed: 18347015]
13. Bruckner K, Perez L, Clausen H, Cohen S. Glycosyltransferase activity of Fringe modulates Notch-Delta interactions. Nature 2000;406:411–415. [PubMed: 10935637]
14. Moloney DJ, Panin VM, Johnston SH, Chen J, Shao L, et al. Fringe is a glycosyltransferase that modifies Notch. Nature 2000;406:369–375. [PubMed: 10935626]
15. Gonzalez de Peredo A, Klein D, Macek B, Hess D, Peter-Katalinic J, et al. C-mannosylation and o-fucosylation of thrombospondin type 1 repeats. Mol Cell Proteomics 2002;1:11–18. [PubMed: 12096136]
16. Ricketts LM, Dlugosz M, Luther KB, Haltiwanger RS, Majerus EM. O-fucosylation is required for ADAMTS13 secretion. J Biol Chem 2007;282:17014–17023. [PubMed: 17395589]

17. Tan K, Duquette M, Liu JH, Dong Y, Zhang R, et al. Crystal structure of the TSP-1 type 1 repeats: a novel layered fold and its biological implication. J Cell Biol 2002;159:373–382. [PubMed: 12391027]
18. Wang LW, Dlugosz M, Somerville RP, Raed M, Haltiwanger RS, et al. O-fucosylation of thrombospondin type 1 repeats in ADAMTS-like-1/punctin-1 regulates secretion: implications for the ADAMTS superfamily. J Biol Chem 2007;282:17024–17031. [PubMed: 17395588]
19. Kozma K, Keusch JJ, Hegemann B, Luther KB, Klein D, et al. Identification and characterization of abeta1,3-glucosyltransferase that synthesizes the Glc-beta1,3-Fuc disaccharide on thrombospondin type 1 repeats. J Biol Chem 2006;281:36742–36751. [PubMed: 17032646]
20. Sato T, Sato M, Kiyohara K, Sogabe M, Shikanai T, et al. Molecular cloning and characterization of a novel human beta1,3-glucosyltransferase, which is localized at the endoplasmic reticulum and glucosylates O-linked fucosylglycan on thrombospondin type 1 repeat domain. Glycobiology 2006;16:1194–1206. [PubMed: 16899492]
21. Hess D, Keusch JJ, Oberstein SA, Hennekam RC, Hofsteenge J. Peters Plus syndrome is a new congenital disorder of glycosylation and involves defective Omicron-glycosylation of thrombospondin type 1 repeats. J Biol Chem 2008;283:7354–7360. [PubMed: 18199743]
22. Lesnik Oberstein SA, Kriek M, White SJ, Kalf ME, Szuhai K, et al. Peters Plus syndrome is caused by mutations in B3GALTL, a putative glycosyltransferase. Am J Hum Genet 2006;79:562–566. [PubMed: 16909395]
23. Fiore R, Rahim B, Christoffels VM, Moorman AF, Puschel AW. Inactivation of the Sema5a gene results in embryonic lethality and defective remodeling of the cranial vascular system. Mol Cell Biol 2005;25:2310–2319. [PubMed: 15743826]
24. Hourcade DE. Properdin and complement activation: a fresh perspective. Curr Drug Targets 2008;9:158–164. [PubMed: 18288967]
25. Jones GC, Riley GP. ADAMTS proteinases: a multi-domain, multi-functional family with roles in extracellular matrix turnover and arthritis. Arthritis Res Ther 2005;7:160–169. [PubMed: 15987500]
26. Kramerova IA, Kawaguchi N, Fessler LI, Nelson RE, Chen Y, et al. Papilin in development; a pericellular protein with a homology to the ADAMTS metalloproteinases. Development 2000;127:5475–5485. [PubMed: 11076767]
27. Leask A, Abraham DJ. All in the CCN family: essential matricellular signaling modulators emerge from the bunker. J Cell Sci 2006;119:4803–4810. [PubMed: 17130294]
28. Meiniel A, Meiniel R, Goncalves-Mendes N, Creveaux I, Didier R, et al. The thrombospondin type 1 repeat (TSR) and neuronal differentiation: roles of SCO-spondin oligopeptides on neuronal cell types and cell lines. Int Rev Cytol 2003;230:1–39. [PubMed: 14692680]
29. Porter S, Clark IM, Kevorkian L, Edwards DR. The ADAMTS metalloproteinases. Biochem J 2005;386:15–27. [PubMed: 15554875]
30. Schubert D, Klar A, Park M, Dargusch R, Fischer WH. F-spondin promotes nerve precursor differentiation. J Neurochem 2006;96:444–453. [PubMed: 16300627]
31. Shiratsuchi T, Nishimori H, Ichise H, Nakamura Y, Tokino T. Cloning and characterization of BAI2 and BAI3, novel genes homologous to brain-specific angiogenesis inhibitor 1 (BAI1). Cytogenet Cell Genet 1997;79:103–108. [PubMed: 9533023]
32. Zhang X, Lawler J. Thrombospondin-based antiangiogenic therapy. Microvasc Res 2007;74:90–99. [PubMed: 17559888]
33. Klar A, Baldassare M, Jessell TM. F-spondin: a gene expressed at high levels in the floor plate encodes a secreted protein that promotes neural cell adhesion and neurite extension. Cell 1992;69:95–110. [PubMed: 1555244]
34. Tortorella M, Pratta M, Liu RQ, Abbaszade I, Ross H, et al. The thrombospondin motif of aggrecanase-1 (ADAMTS-4) is critical for aggrecan substrate recognition and cleavage. J Biol Chem 2000;275:25791–25797. [PubMed: 10827174]
35. Tzarfaty-Majar V, Lopez-Alemany R, Feinstein Y, Gombau L, Goldshmidt O, et al. Plasmin-mediated release of the guidance molecule F-spondin from the extracellular matrix. J Biol Chem 2001;276:28233–28241. [PubMed: 11359777]

36. Dawson DW, Pearce SF, Zhong R, Silverstein RL, Frazier WA, et al. CD36 mediates the In vitro inhibitory effects of thrombospondin-1 on endothelial cells. J Cell Biol 1997;138:707–717. [PubMed: 9245797]
37. Iruela-Arispe ML, Lombardo M, Krutzsch HC, Lawler J, Roberts DD. Inhibition of angiogenesis by thrombospondin-1 is mediated by 2 independent regions within the type 1 repeats. Circulation 1999;100:1423–1431. [PubMed: 10500044]
38. Jimenez B, Volpert OV, Crawford SE, Febbraio M, Silverstein RL, et al. Signals leading to apoptosis-dependent inhibition of neovascularization by thrombospondin-1. Nat Med 2000;6:41–48. [PubMed: 10613822]
39. Volpert OV, Zaichuk T, Zhou W, Reiher F, Ferguson TA, et al. Inducer-stimulated Fas targets activated endothelium for destruction by anti-angiogenic thrombospondin-1 and pigment epithelium-derived factor. Nat Med 2002;8:349–357. [PubMed: 11927940]
40. Arnold SJ, Robertson EJ. Making a commitment: cell lineage allocation and axis patterning in the early mouse embryo. Nat Rev Mol Cell Biol 2009;10:91–103. [PubMed: 19129791]
41. Rozario T, Desimone DW. The extracellular matrix in development and morphogenesis: A dynamic view. Dev Biol. 2009
42. Wang Y, Lee GF, Kelley RF, Spellman MW. Identification of a GDP-L-fucose:polypeptide fucosyltransferase and enzymatic addition of O-linked fucose to EGF domains. Glycobiology 1996;6:837–842. [PubMed: 9023546]
43. Maretto S, Cordenonsi M, Dupont S, Braghetta P, Broccoli V, et al. Mapping Wnt/beta-catenin signaling during mouse development and in colorectal tumors. Proc Natl Acad Sci U S A 2003;100:3299–3304. [PubMed: 12626757]
44. Hogan, B.; Beddington, B.; Costantini, F.; Lacy, E. Manipulating the Mouse Embryo: A Laboratory Manual. New York: Cold Spring Harbor Laboratory press; 1994. p. 373-375.
45. Shumacher A, Faust C, Magnuson T. Positional cloning of a global regulator of anterior-posterior patterning in mice. Nature 1996;383:250–253. [PubMed: 8805699]
46. Nagy, A.; Gertsenstein, M.; Vintersten, K.; Behringer, RR. Manipulating the Mouse Embryo: A Laboratory Manual. Cold Spring Harbor Laboratory Press; 2003. p. 31-141.
47. O'Brien BR. Development of haemoglobin by de-embryonated chick blastoderms cultured in vitro and the effect of abnormal RNA upon its synthesis. J Embryol Exp Morphol 1961;9:202–221. [PubMed: 13730007]
48. Wiggins CA, Munro S. Activity of the yeast MNN1 alpha-1,3-mannosyltransferase requires a motif conserved in many other families of glycosyltransferases. Proc Natl Acad Sci U S A 1998;95:7945–7950. [PubMed: 9653120]
49. Adams JC, Tucker RP. The thrombospondin type 1 repeat (TSR) superfamily: diverse proteins with related roles in neuronal development. Dev Dyn 2000;218:280–299. [PubMed: 10842357]
50. Mitchell KJ, Pinson KI, Kelly OG, Brennan J, Zupicich J, et al. Functional analysis of secreted and transmembrane proteins critical to mouse development. Nat Genet 2001;28:241–249. [PubMed: 11431694]
51. Belaoussoff M, Farrington SM, Baron MH. Hematopoietic induction and respecification of A-P identity by visceral endoderm signaling in the mouse embryo. Development 1998;125:5009–5018. [PubMed: 9811585]
52. Ema M, Takahashi S, Rossant J. Deletion of the selection cassette, but not cis-acting elements, in targeted Flk1-lacZ allele reveals Flk1 expression in multipotent mesodermal progenitors. Blood 2006;107:111–117. [PubMed: 16166582]
53. Tremblay KD, Dunn NR, Robertson EJ. Mouse embryos lacking Smad1 signals display defects in extra-embryonic tissues and germ cell formation. Development 2001;128:3609–3621. [PubMed: 11566864]
54. Kabrun N, Buhring HJ, Choi K, Ullrich A, Risau W, et al. Flk-1 expression defines a population of early embryonic hematopoietic precursors. Development 1997;124:2039–2048. [PubMed: 9169850]
55. Yamaguchi TP, Dumont DJ, Conlon RA, Breitman ML, Rossant J. flk-1, an flt-related receptor tyrosine kinase is an early marker for endothelial cell precursors. Development 1993;118:489–498. [PubMed: 8223275]

56. Motoike T, Markham DW, Rossant J, Sato TN. Evidence for novel fate of Flk1+ progenitor: contribution to muscle lineage. Genesis 2003;35:153–159. [PubMed: 12640619]
57. Brennan J, Lu CC, Norris DP, Rodriguez TA, Beddington RS, et al. Nodal signalling in the epiblast patterns the early mouse embryo. Nature 2001;411:965–969. [PubMed: 11418863]
58. Camus A, Perea-Gomez A, Moreau A, Collignon J. Absence of Nodal signaling promotes precocious neural differentiation in the mouse embryo. Dev Biol 2006;295:743–755. [PubMed: 16678814]
59. Fuentealba LC, Eivers E, Ikeda A, Hurtado C, Kuroda H, et al. Integrating patterning signals: Wnt/GSK3 regulates the duration of the BMP/Smad1 signal. Cell 2007;131:980–993. [PubMed: 18045539]
60. Abreu JG, Ketpura NI, Reversade B, De Robertis EM. Connective-tissue growth factor (CTGF) modulates cell signalling by BMP and TGF-beta. Nat Cell Biol 2002;4:599–604. [PubMed: 12134160]
61. Gupta K, Gupta P, Wild R, Ramakrishnan S, Hebbel RP. Binding and displacement of vascular endothelial growth factor (VEGF) by thrombospondin: effect on human microvascular endothelial cell proliferation and angiogenesis. Angiogenesis 1999;3:147–158. [PubMed: 14517432]
62. Luque A, Carpizo DR, Iruela-Arispe ML. ADAMTS1/METH1 inhibits endothelial cell proliferation by direct binding and sequestration of VEGF165. J Biol Chem 2003;278:23656–23665. [PubMed: 12716911]
63. Nakamura Y, Weidinger G, Liang JO, Aquilina-Beck A, Tamai K, et al. The CCN family member Wisp3, mutant in progressive pseudorheumatoid dysplasia, modulates BMP and Wnt signaling. J Clin Invest 2007;117:3075–3086. [PubMed: 17823661]
64. Rodriguez-Manzaneque JC, Lane TF, Ortega MA, Hynes RO, Lawler J, et al. Thrombospondin-1 suppresses spontaneous tumor growth and inhibits activation of matrix metalloproteinase-9 and mobilization of vascular endothelial growth factor. Proc Natl Acad Sci U S A 2001;98:12485–12490. [PubMed: 11606713]
65. Suga A, Hikasa H, Taira M. Xenopus ADAMTS1 negatively modulates FGF signaling independent of its metalloprotease activity. Dev Biol 2006;295:26–39. [PubMed: 16690049]
66. Le Goff C, Morice-Picard F, Dagoneau N, Wang LW, Perrot C, et al. ADAMTSL2 mutations in geleophysic dysplasia demonstrate a role for ADAMTS-like proteins in TGF-beta bioavailability regulation. Nat Genet 2008;40:1119–1123. [PubMed: 18677313]
67. Ben-Haim N, Lu C, Guzman-Ayala M, Pescatore L, Mesnard D, et al. The nodal precursor acting via activin receptors induces mesoderm by maintaining a source of its convertases and BMP4. Dev Cell 2006;11:313–323. [PubMed: 16950123]
68. Iratni R, Yan YT, Chen C, Ding J, Zhang Y, et al. Inhibition of excess nodal signaling during mouse gastrulation by the transcriptional corepressor DRAP1. Science 2002;298:1996–1999. [PubMed: 12471260]
69. Hogan BL, Cooper AR, Kurkinen M. Incorporation into Reichert's membrane of laminin-like extracellular proteins synthesized by parietal endoderm cells of the mouse embryo. Dev Biol 1980;80:289–300. [PubMed: 7450285]
70. Leivo I, Vaheri A, Timpl R, Wartiovaara J. Appearance and distribution of collagens and laminin in the early mouse embryo. Dev Biol 1980;76:100–114. [PubMed: 6991310]
71. Wartiovaara J, Leivo I, Vaheri A. Expression of the cell surface-associated glycoprotein, fibronectin, in the early mouse embryo. Dev Biol 1979;69:247–257. [PubMed: 376373]
72. Dzamba BJ, Jakab KR, Marsden M, Schwartz MA, DeSimone DW. Cadherin adhesion, tissue tension, and noncanonical Wnt signaling regulate fibronectin matrix organization. Dev Cell 2009;16:421–432. [PubMed: 19289087]
73. Dyer MA, Farrington SM, Mohn D, Munday JR, Baron MH. Indian hedgehog activates hematopoiesis and vasculogenesis and can respecify prospective neurectodermal cell fate in the mouse embryo. Development 2001;128:1717–1730. [PubMed: 11311154]
74. Nakazawa F, Nagai H, Shin M, Sheng G. Negative regulation of primitive hematopoiesis by the FGF signaling pathway. Blood 2006;108:3335–3343. [PubMed: 16888091]
75. Vazquez F, Hastings G, Ortega MA, Lane TF, Oikemus S, et al. METH-1, a human ortholog of ADAMTS-1, and METH-2 are members of a new family of proteins with angio-inhibitory activity. J Biol Chem 1999;274:23349–23357. [PubMed: 10438512]

76. Bornstein P, Agah A, Kyriakides TR. The role of thrombospondins 1 and 2 in the regulation of cell-matrix interactions, collagen fibril formation, and the response to injury. Int J Biochem Cell Biol 2004;36:1115–1125. [PubMed: 15094126]
77. Feinstein Y, Klar A. The neuronal class 2 TSR proteins F-spondin and Mindin: a small family with divergent biological activities. Int J Biochem Cell Biol 2004;36:975–980. [PubMed: 15094111]
78. Hirohata S, Wang LW, Miyagi M, Yan L, Seldin MF, et al. Punctin, a novel ADAMTS-like molecule, ADAMTSL-1, in extracellular matrix. J Biol Chem 2002;277:12182–12189. [PubMed: 11805097]
79. Holbourn KP, Acharya KR, Perbal B. The CCN family of proteins: structure-function relationships. Trends Biochem Sci 2008;33:461–473. [PubMed: 18789696]
80. Tucker RP. The thrombospondin type 1 repeat superfamily. Int J Biochem Cell Biol 2004;36:969–974. [PubMed: 15094110]
81. Xu X, Dong C, Vogel BE. Hemicentins assemble on diverse epithelia in the mouse. J Histochem Cytochem 2007;55:119–126. [PubMed: 17015624]
82. Yang Z, Strickland DK, Bornstein P. Extracellular matrix metalloproteinase 2 levels are regulated by the low density lipoprotein-related scavenger receptor and thrombospondin 2. J Biol Chem 2001;276:8403–8408. [PubMed: 11113133]
83. Shukla S, Nair R, Rolle MW, Braun KR, Chan CK, et al. Synthesis and organization of hyaluronan and versican by embryonic stem cells undergoing embryoid body differentiation. J Histochem Cytochem 2010;58:345–358. [PubMed: 20026669]
84. Glasson SS, Askew R, Sheppard B, Carito B, Blanchet T, et al. Deletion of active ADAMTS5 prevents cartilage degradation in a murine model of osteoarthritis. Nature 2005;434:644–648. [PubMed: 15800624]
85. Glasson SS, Askew R, Sheppard B, Carito BA, Blanchet T, et al. Characterization of and osteoarthritis susceptibility in ADAMTS-4-knockout mice. Arthritis Rheum 2004;50:2547–2558. [PubMed: 15334469]
86. Lawler J, Sunday M, Thibert V, Duquette M, George EL, et al. Thrombospondin-1 is required for normal murine pulmonary homeostasis and its absence causes pneumonia. J Clin Invest 1998;101:982–992. [PubMed: 9486968]
87. Majumdar MK, Askew R, Schelling S, Stedman N, Blanchet T, et al. Double-knockout of ADAMTS-4 and ADAMTS-5 in mice results in physiologically normal animals and prevents the progression of osteoarthritis. Arthritis Rheum 2007;56:3670–3674. [PubMed: 17968948]
88. Chen Y, Abraham DJ, Shi-Wen X, Pearson JD, Black CM, et al. CCN2 (connective tissue growth factor) promotes fibroblast adhesion to fibronectin. Mol Biol Cell 2004;15:5635–5646. [PubMed: 15371538]
89. Irvine AE, Perbal B, Yeger H. Report on the fifth international workshop on the CCN family of genes. J Cell Commun Signal 2008;2:95–100. [PubMed: 19156540]
90. Heath E, Tahri D, Andermarcher E, Schofield P, Fleming S, et al. Abnormal skeletal and cardiac development, cardiomyopathy, muscle atrophy and cataracts in mice with a targeted disruption of the Nov (Ccn3) gene. BMC Dev Biol 2008;8:18. [PubMed: 18289368]
91. Ivkovic S, Yoon BS, Popoff SN, Safadi FF, Libuda DE, et al. Connective tissue growth factor coordinates chondrogenesis and angiogenesis during skeletal development. Development 2003;130:2779–2791. [PubMed: 12736220]
92. Kutz WE, Gong Y, Warman ML. WISP3, the gene responsible for the human skeletal disease progressive pseudorheumatoid dysplasia, is not essential for skeletal function in mice. Mol Cell Biol 2005;25:414–421. [PubMed: 15601861]
93. Hurvitz JR, Suwairi WM, Van Hul W, El-Shanti H, Superti-Furga A, et al. Mutations in the CCN gene family member WISP3 cause progressive pseudorheumatoid dysplasia. Nat Genet 1999;23:94–98. [PubMed: 10471507]
94. Mo FE, Muntean AG, Chen CC, Stolz DB, Watkins SC, et al. CYR61 (CCN1) is essential for placental development and vascular integrity. Mol Cell Biol 2002;22:8709–8720. [PubMed: 12446788]
95. Wang LW, Leonhard-Melief C, Haltiwanger RS, Apte SS. Post-translational modification of thrombospondin type-1 repeats in ADAMTS-like 1/punctin-1 by C-mannosylation of tryptophan. J Biol Chem 2009;284:30004–30015. [PubMed: 19671700]

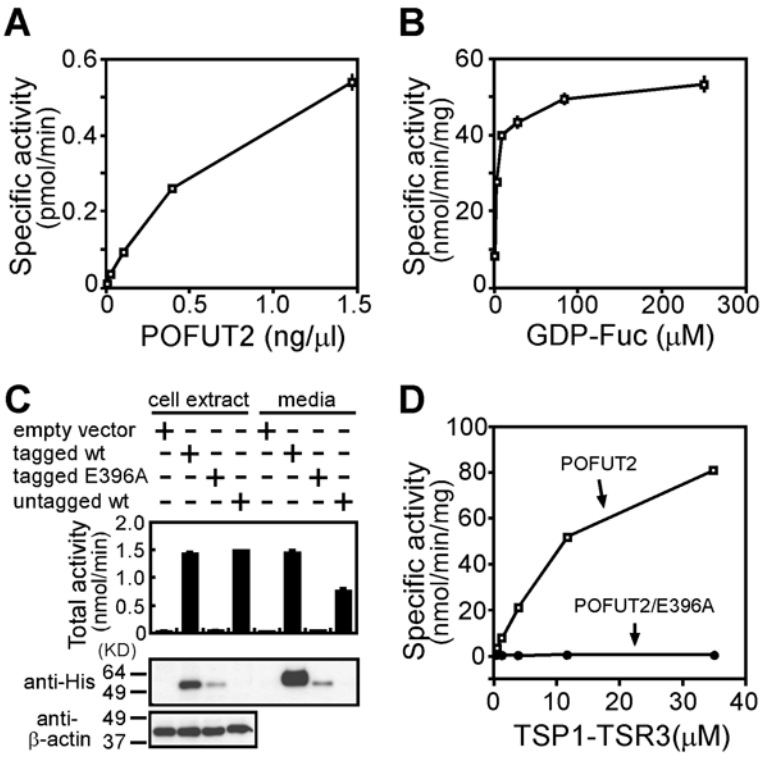

Figure 1. Mouse POFUT2 specifically transferred fucose to TSRs

TSR-specific *O*-fucosyltransferase activity of mouse POFUT2 is dependent on (A) enzyme concentration and (B) GDP-fucose concentration. (C) The POFUT2 ERE motif is essential for POFUT2 activity. HEK293T cells were transiently transfected with empty pcDNA4 vector (lane 1 and 5), expression plasmids for *Pofut2-myc-His* (lane 2 and 6), *Pofut2/E396A-myc-His* in which the ERE motif had been mutated (lane 3 and 7), and wildtype untagged *Pofut2* (lane 4 and 8). The cell extracts (lanes 1 to 4) and the culture media (lanes 5 to 8) were assayed for TSR-specific *O*-fucosyltransferase activity using TSP1-TSR3 as acceptor substrate (top panel). POFUT2-myc-His expression levels were detected by Western blot of cell extracts and culture media using anti-His antibody (His-probe (H-15), SantaCruz) (middle panel). β-actin expression provided a loading control in the bottom panel. (D) Mouse POFUT2 activity is dependent upon TSP1-TSR3 concentration. No activity was observed for POFUT2/E396A-myc-His. Each assay contained 1.5 ng of purified POFUT2-myc-His (open squares) or POFUT2/E396A-myc-His (filled circles) and increasing concentration of TSP1-TSR3. All the POFUT2 assays were performed in duplicate. Error bars represent the spread of the data.

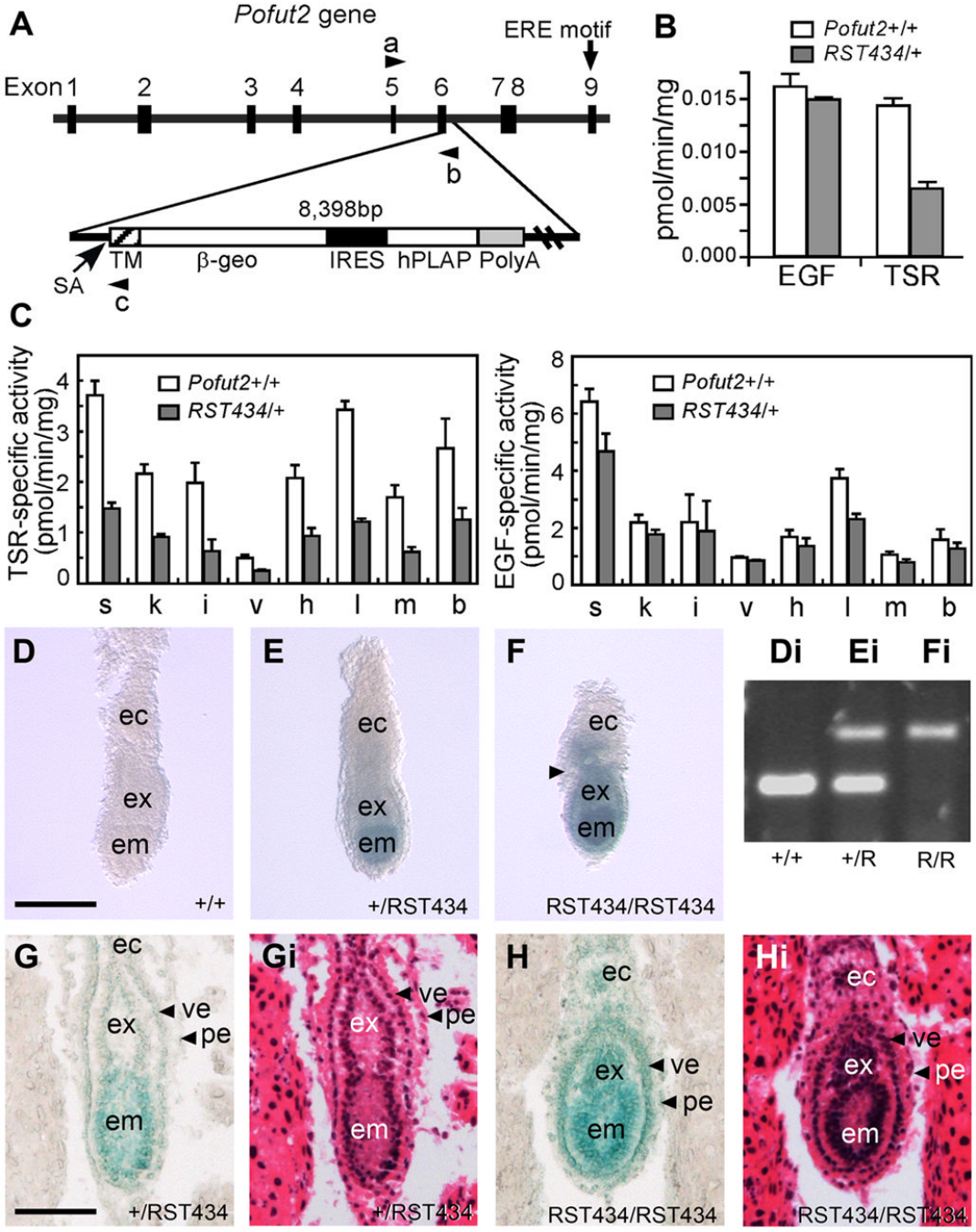

Figure 2. *Pofut2* was essential for epithelial organization in the early gastrula

(A) (Above) Diagram of the mouse *Pofut2* exon and intron structure; the ERE motif required for POFUT2 enzymatic activity resides in exon 9. In the *RST434* line, the pGT0TMpfs genetrap inserted in exon 6 and was accompanied by a 38 bp deletion. A splice acceptor (SA) site is located upstream of the transmembrane domain (TM) and β-galactosidase-neomycin phosphotransferase fusion (β-geo). Arrowheads indicate primers used for genotyping: a, RST434-forward; b, RST434-reverse1; c, RST434-reverse2. IRES, internal ribosome entry site; hPLAP, human placental alkaline phosphatase; PolyA, polyadenylation signal. (B) Extracts of *RST434* heterozygous and *wildtype* ES cells were assayed for POFUT1 and POFUT2 activity using Factor VII EGF repeat (EGF) and the third thrombospondin type 1

repeat of TSP1 (TSR), respectively, as acceptor substrates. (C) Protein *O*-fucosyltransferase assays were performed with tissue extracts obtained from 5-week-old *wildtype* (n=4, open bars) and heterozygous *RST434* (n=4, filled bars) mice using TSP1-TSR3 to detect POFUT2 activity (Right) or EGF repeats to detect POFUT1 activity (Left). Total protein was obtained from spleen, s; kidney, k; intestine, i; liver, v; heart, h; lung, l; muscle, m; and brain, b. Values were shown as means ± S.E. (D–F) Embryos stained for LacZ activity from *RST434* heterozygous intercross at E 6.5. Constriction between the ectoplacental cone and extraembryonic ectoderm is indicated by arrowhead in panel F. The distal halves of the embryos were then dissected for genotyping (Di–Fi). The lower amplified band represents the wild-type *Pofut2* allele (primers a and b), and the upper band the *RST434* allele (primers a and c). (G, H) Histological analysis of embryos at E 6.5. Heterozygous (G) and homozygous (H) littermates stained for LacZ activity, sectioned and photographed (G, H), then stained with hematoxylin and eosin Y (Gi, Hi). Number of mutant embryos represented by panels: F (8), H (8). Proximal is up; distal is down. Abbreviations: ec, ectoplacental cone; em, embryonic ectoderm; ex, extraembryonic ectoderm; pe, parietal endoderm; ve, visceral endoderm.

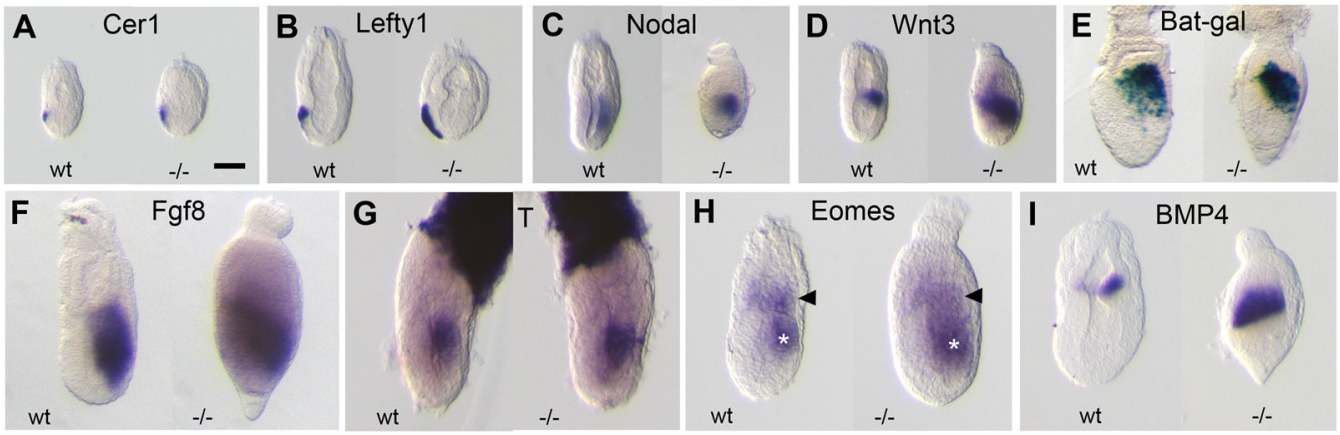

Figure 3. Loss of *Pofut2* resulted in expanded expression of early primitive streak markers

(A–D, F–I) Whole mount *in situ* hybridization was used to examine gene expression in *Wildtype* (wt) and *RST434* homozygous littermates (−/−) dissected at E6.5 (*Cer*, *Lefty1*, *Nodal*, *Wnt*, *Eomes*, and *T*) or E7.0 (*Fgf8*, *BMP4*), using the indicated probes. (E) Wnt signaling activity was measured in E 7.0 *699Lex wildtype* and homozygous mutant embryos, using the BAT-gal transgene reporter [43]. Anterior is to the left; posterior is to the right. Number of mutant embryos represented by panels: *Cer1* (4), *Lefty1* (4), *Nodal* (6), *Wnt3* (6), *Bat-gal* (10), *Fgf8* (15), *T* (3), *Eomes* (3), *BMP4* (7). Proximal is up; distal is down. Scale bar indicates 100 μm.

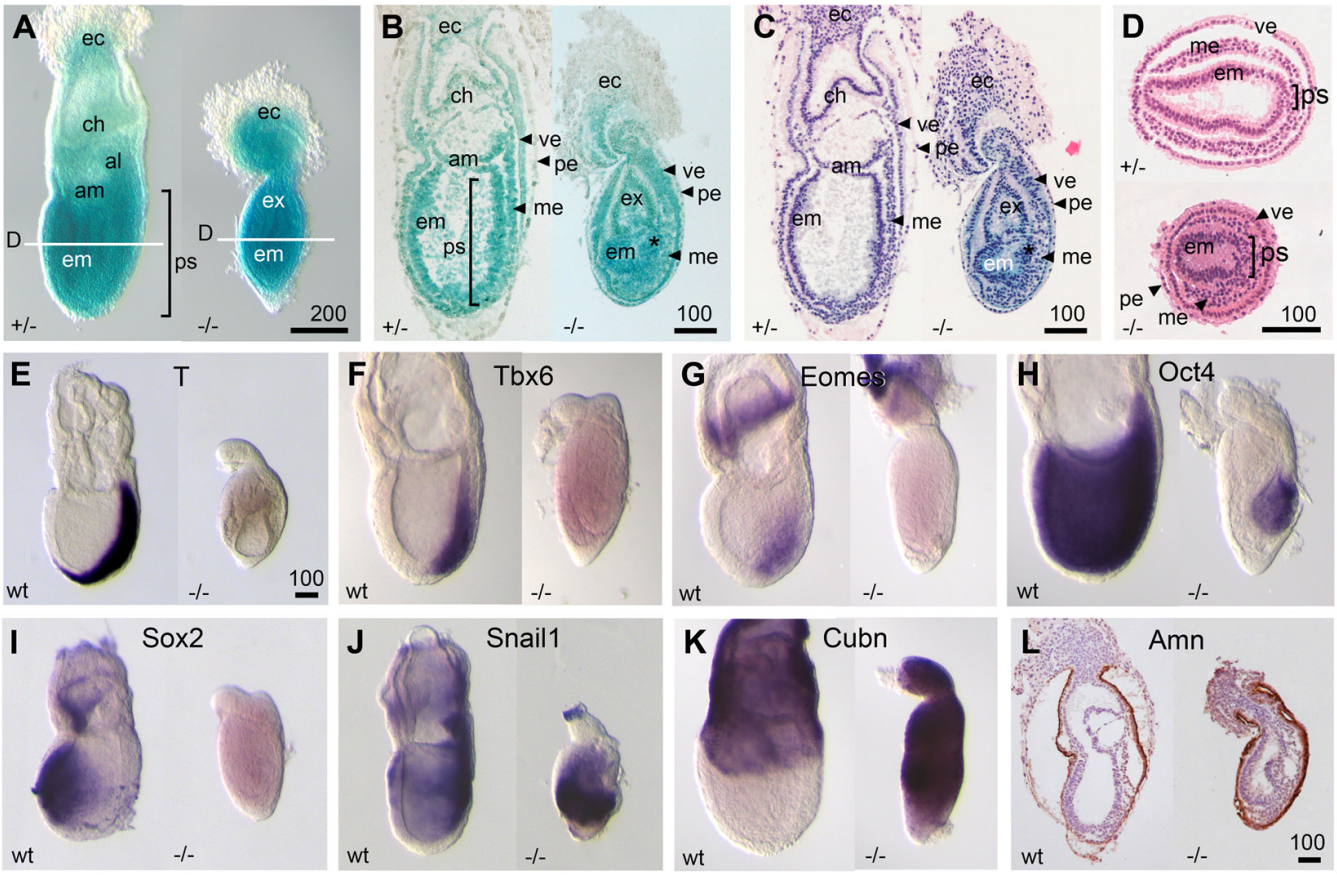

Figure 4. Primitive streak and proximal visceral endoderm were expanded in *Pofut2* mutants

(A) Whole-Mount and (B–D) histological analysis of E 7.5 embryos dissected from *RST434* heterozygous intercross. Embryos were stained for LacZ activity, sectioned and photographed (B), then stained with hematoxylin and eosin Y (C, D). (B–C) Sagittal sections (D) Transverse embryo sections were isolated from the epiblast midpoint; the approximate plane of transverse sections is indicated by white line in panel A. al, allantois; am, amnion; ch, chorion; ec, ectoplacental cone; em, embryonic ectoderm; ex, extra-embryonic ectoderm; me, embryonic mesoderm; pe, parietal endoderm; ps, primitive streak; ve, visceral endoderm. Bracket indicates primitive streak. Scale bar = 100 μm. (E–K) Whole mount in situ hybridization was used to examine gene expression in *wildtype* (wt) and *RST434* homozygous littermates (−/−) using the indicated probes. (L) Distribution of Amnionless in the visceral endoderm was analyzed by immunohistochemistry. Number of mutant embryos represented by panels: A (7), B (8), C (10), D (5), *T* (9), *Tbx6* (3), *Eomes* (4), *Oct4* (5), *Sox2* (3), *Snail1* (10), *Cubn* (5), Amn (3). Anterior is left; posterior is right. Proximal is up; distal is down. Scale bar size is indicated in μm.

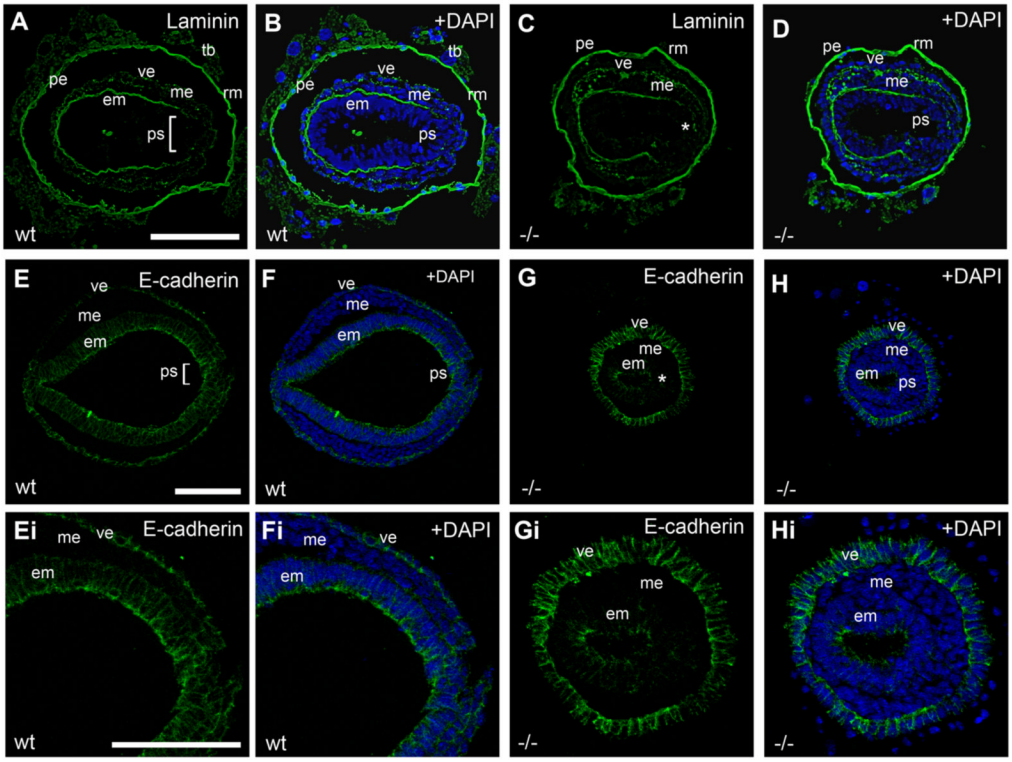

Figure 5. Loss of *Pofut2* resulted in expanded EMT

(A–H) Immunofluorescence analysis of E 7.5 wildtype (A–B, E–F) and *RST434* mutant (C–D, G–H) embryos stained with anti-Laminin (Green) (n=3) (A–D) or anti-E-cadherin (Green) (n=3) antibody (E–H). Panels Ei–Hi represent higher magnification of sections shown in E–H. E-cadherin (Green) was dramatically down regulated in the mutant embryonic ectoderm. Nuclei are visualized with DAPI (Blue). White bracket and asterisk denotes the primitive streak in *wild type* embryos and *Pofut2* mutant embryos, respectively. em, embryonic ectoderm; me, mesoderm; pe, parietal endoderm; ps, primitive streak; rm, Reichert's membrane; tb, trophoblast; ve, visceral endoderm. Anterior is left; posterior is right. Scale bars sizes are indicated in μm.

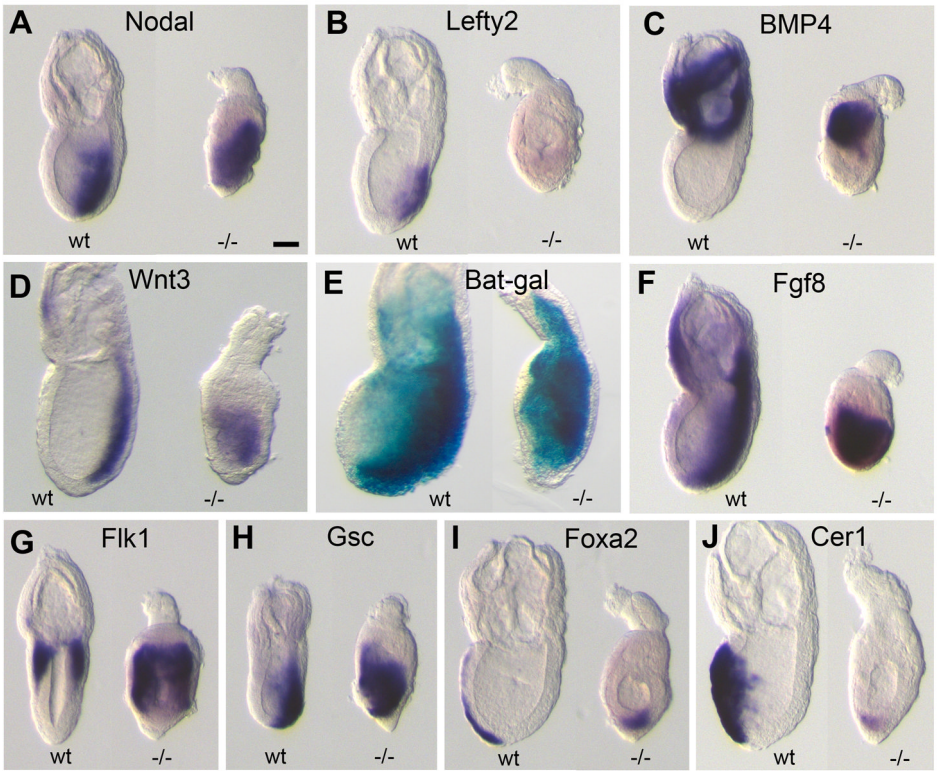

Figure 6. Loss of *Pofut2* resulted in expanded expression of major growth factor signaling molecules

(A–D and F–I) Whole mount *in situ* hybridization was used to examine gene expression in E7.5 *wildtype* (wt) and *RST434* homozygous littermates (−/−) using the indicated probes. (E) Wnt signaling activity was measured in *wildtype* and *699Lex* homozygous embryos with one copy of the BAT-gal transgene reporter [43]. Wnt activity is expanded toward the anterior (left) in *Pofut2* mutants. Number of mutant embryos represented by panels: *Nodal* (6), *Lefty2* (3), *BMP4* (4), *Wnt3* (6), *Bat-gal* (9), *Fgf8* (5), *Flk1* (10), *Gsc* (7), *Foxa2* (8), *Cer1* (3). Anterior is to the left; posterior is to the right. Proximal is up; distal is down. Scale bar indicates 100 μm.

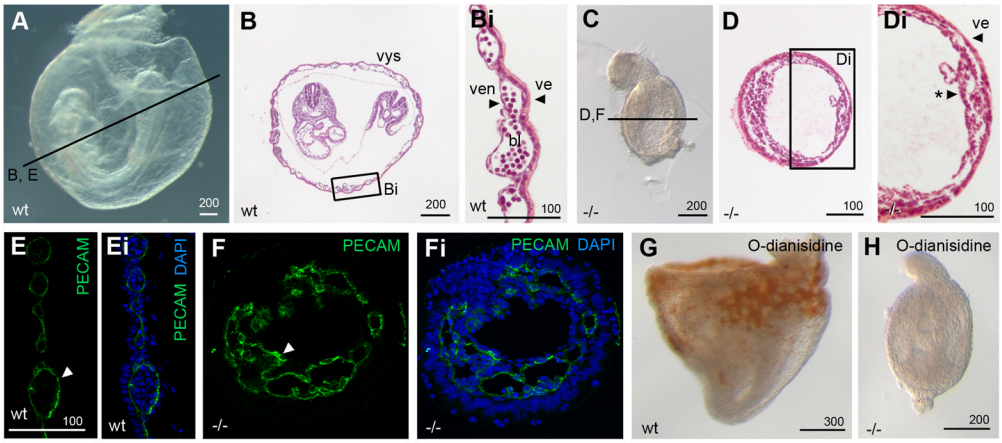

Figure 7. Mesoderm in *Pofut2* mutants preferentially differentiates into vascular endothelial cells

(A–Di) Whole mount and (B and D) transverse hematoxylin and eosin Y stained sections of E 8.5 wildtype (A–Bi) and *Pofut2* mutant (C–Di) embryos. (E–Fi) Immunofluorescence staining with PECAM antibody (green indicated by white arrowhead) and DAPI (blue) in E 8.5 control (E–Ei) and *RST434* mutant littermates (F–Fi). Approximate plane of sectioning for panels (B, D–G) are indicated by black lines in A and C. Bi and Di represent enlargements of boxed regions in panel B and D. (G, H) O-dianisidine staining of E 8.5 wild type (G) and mutant (H) embryos. Number of mutant embryos represented by panels: C (9), D (7), PECAM (9), O-dianisidine (6). For panels A–D and G and H anterior is left; posterior is right. Proximal is up; distal is down. Abbreviations: bl, primitive erythrocytes; ve, visceral endoderm; ven, vascular endothelial cells; *, condensed mesoderm. Scale bar sizes indicated in μm.

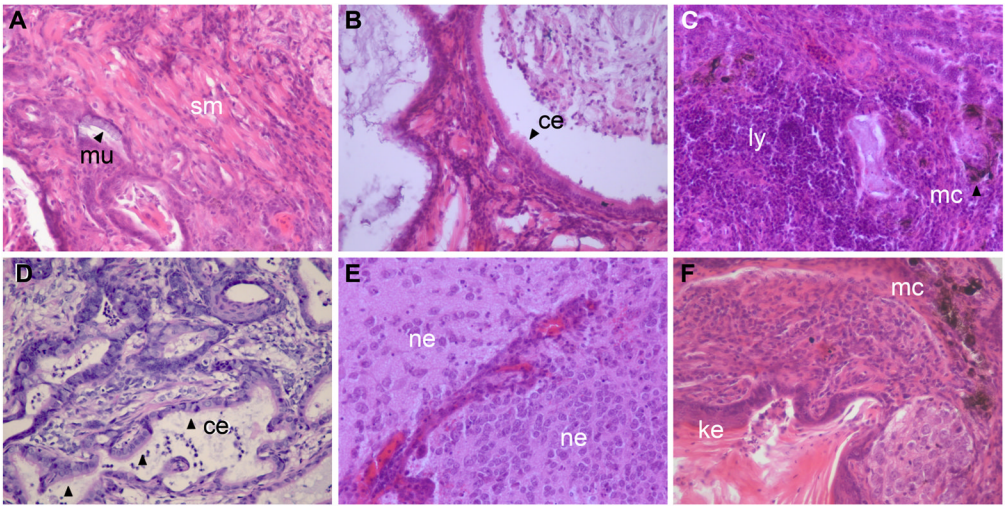

Figure 8. The inability of *Pofut2* mutant embryos to form differentiated tissues derived from all three germ layers was rescued in teratomas

(A–F) Teratomas (n=6) derived from E 7.5 *Pofut2* mutant embryos were sectioned and stained with hematoxylin and eosin Y. Tumors were comprised of tissues derived from all three germ layers. Endoderm derived tissues include mucin-producing columnar epithelial cells (mu), and ciliated respiratory epithelial-type columnar cells (ce). Ectoderm derived tissues include neural epithelium (ne), keratinized squamous cells (ke), and melanocytes (mc). Smooth muscle (sc) and lymphoid tissue (ly) are derived from mesoderm.

Table 1

Mouse Proteins with putative O-fucosylation site within TSRs*

TSR class	Mouse Protein	# Consensus Sequences	Family
Group 1	ADAMTS1-4, ADAMTS5 [95], ADAMTS6-10, ADAMTS12, ADAMTS13 [16], ADAMTS14-20	1–12	a disintegrin and metalloproteinase with thrombospondin motifs (ADAMTS)
	ADAMTSL1 [18,95], ADAMTSL2-6	1–10	ADAMTS-like
	BAI1-3	4	brain-specific angiogenesis inhibitor
	Cfp (Properdin) [15]	4	complement component
	CILP2	1	cartilage intermediate layer protein/nucleotide pyrophosphohydrolase
	HMCN1	6	hemicentin
	PAPLN (Papilin)	4	
	SEMA5A, SEMA5b	2	semaphorin
	THBS1 (TSP-1) [1,15], THBS2(TSP-2)	3	thrombospondin
	ISM1, ISM2, XM_283765	1	isthmin
	UNC5a	1	UNC5
Group1 and Group 2	C6	1	complement component
	SSPO (Sco-spondin)	12	spondin
	THSD7a, THSD7b	4–5	thrombospondin, type I, domain-containing
Group 2	CCN1 (CYR61), CCN2 (CTGF), CCN3 (NOV), CCN4(ELM1/WISP1), CCN5(COP1/WISP2), CCN6 (WISP3)	1	CCN (Cyr61, Ctgf, Nov)
	SPON1 (f-spondin) [15]	4	spondin

*Fifty-one proteins that contain the consensus sequence $CX_{(2–3)}S/TCX_{(2)}G$ within TSRs are listed above as putative POFUT2 targets and are divided into groups 1or 2 based on their TSR structures (Tan et al., 2002). Underlined proteins indicate Human, mouse, or rat homologues of verified to contain O-fucosylated TSRs. Mouse proteins containing TSRs were identified by searching SMART database (http://smart.embl-heidelberg.de/) with keyword TSP1 in both normal and genomic modes. Alternative protein names are listed in parentheses.

Table 2

Disruption of *Pofut2* gene resulted in embryonic lethality by E 10.5

		genotype					
Cross	**Stage examined**	**Wt**	**Het**	**Hm**	**Res sites**	**Litter total**	**% Hm (p)**
RST434 × *RST434*[*]	P 15	35	60	0		95	0
RST434 × *RST434*[**]	E 10.5	18	43	0	19	80	23.8 (0.79)
RST434 × *RST434*[#]	E 7.5	18	27	15	0	60	25 (1.00)
RST434 × *RST434*[#]	E 6.5	11	27	13	0	51	25.5 (0.94)
RST434 × *699Lex*[$]	E 7.5	ND	ND	14	0	52	26.9 (0.75)
699Lex × *699Lex*[$]	E 7.5	ND	ND	29	0	114	25.4 (0.91)

[*] Genotype determined by PCR (Materials and Methods)

[**] Resorption sites (Res sites) were counted and surviving embryos genotyped by PCR.

[#] Genotypes were inferred from the intensity of X-gal staining and embryo morphology. The relationship between these characteristics and genotype was verified by PCR (Materials and Methods).

[$] homozygous genotype inferred from mutant morphology. Wt, wild type; Het, heterozygous; Hm, homozygous; nd, not determined.